RELATIONSHIP BETWEEN SNOW EXTENT AND MID-LATITUDE CYCLONE CENTERS FROM NARR OBJECTIVELY DERIVED STORM POSITION AND SNOW COVER

by

Matthew Rydzik

A thesis submitted in partial fulfillment of

the requirements for the degree of

Master of Science

(Atmospheric and Oceanic Sciences)

at the

UNIVERSITY OF WISCONSIN - MADISON

2012

APPROVED

Signature

Date

Ankur R. Desai, Ph.D.
Associate Professor
University of Wisconsin - Madison
Department of Atmospheric and Oceanic Sciences

Abstract

A relationship between mid-latitude cyclone (MLC) tracks and snow cover extent has been discussed in the literature over the last 50 years, but not explicitly analyzed with high-resolution and long-term observations of both. Large-scale modeling studies have hinted that areas near the edge of the snow extent support enhanced baroclinicity due to differences in surface albedo and moisture fluxes. In this study, we investigated the relationship between snow cover extent and MLC trajectories across North America using objectively analyzed mid-latitude storm trajectories and snow cover extent from the North American Regional Reanalysis (NARR) for 1979 to 2010. We developed a high-resolution MLC database from sea-level pressure minima that are tracked through subsequent three hour time steps and we developed a simple algorithm that identified the southern edge of the snow cover extent. We find a robust enhanced frequency of MLCs in a region 50-350 km south of the snow cover extent. The region of enhanced MLC frequency coincides with the region of maximum low-level baroclinicity. These observations support hypotheses of an internal feedback in which the snow cover extent is leading the storm tracks through surface heat and moisture fluxes. Further, these results aid in the understanding of how mid-latitude cyclone tracks will shift in a changing climate in response to snow cover trends.

Acknowledgments

First and foremost, I want to thank my research and academic advisor, Associate Professor Ankur Desai. Without his initial idea, insightful discussions, and support none of this work would have been possible. I also need to extend my gratitude to my fellow lab mates and lab support staff for their helpful comments on figures and presentations over the last two years. I thank my thesis readers, Professor Jonathan Martin and Associate Professor Dan Vimont, for comments on this document. I would also like to thank my fellow graduate students who have made the last two years in Madison very enjoyable. Lastly, I need to thank my girlfriend, Mallie Toth, for providing support throughout my two years in graduate school, inciting intellectual discussions about my research, and for proofreading an early draft of this thesis.

This work was funded by the USA Department of Energys 20% By 2030 Award Number, DE-EE0000544/001, titled 'Integration of Wind Energy Systems into Power Engineering Education Programs at UW-Madison.'

Contents

List of Figures

List of Tables

1 Introduction

Trajectories of mid-latitude cyclones (MLCs) are important for both climate and weather prediction because they have a direct impact on the weather that people experience every day. MLCs are primarily driven by large scale forcing such as upper-level jets and baroclinic instability. It can be argued, however, that boundary layer forcing may play a role in some MLC trajectories by the modulation of boundary layer thermodynamics. Individual case studies are useful for showing the mechanistic process that modulation of the boundary layer can have on the atmosphere, but only large scale statistical analysis can determine if these processes actually occur. This thesis focuses on the relationship between pre-existing snow cover and MLC trajectories.

1.1 Motivation

A relationship between snow cover extent and MLCs has been discussed in the literature for almost 50 years; however, it has not been explicitly analyzed with high-resolution and long-term observations of both. A relationship between the two is believed to exist because of the significant impact snow cover has on the surface energy balance through its insulating properties and high albedo. Albedo is the proportion of incident radiation that is reflected by a surface (Wallace and Hobbs, 2006). Typically, over land, albedo is the fraction of incident solar radiation that is reflected back toward space. Heating of the atmosphere is primarily driven though solar radiation that is absorbed by the land surface and re-emitted as sensible heat and convection (Wallace and Hobbs, 2006). Therefore, surface albedo plays a strong role in atmospheric heating because it controls how much energy is input into the system. In addition, the amount of absorbed radiation at the surface impacts the amount of sensible and latent heat fluxes from the surface. Modification of absorbed surface radiation, latent heat flux, and sensible heat flux will have a significant impact on the overlying atmosphere (Ellis and Leathers, 1998). Snow

cover, through its high albedo and insulation effects, is known to have significant climate implications through temperature and energy balance (Cohen and Rind, 1991; Vavrus, 2007).

Namias (1962) was one of the first to suggest a direct relationship between MLC trajectories and pre-existing snow cover. Using the abnormal southern extent of snow from February to March of 1960, Namias showed an anomalous climatological high pressure over much of North America. This is indicative of repeat MLCs developing off the east coast of North America (Namias, 1962). Estimating surface air temperature from mid-level geopotential height, Namias showed that the largest difference between the estimated surface temperature and observed surface temperature occurred along the southern edge of the snow extent, with the difference reaching up to 5.6°C. The finding suggests that snow cover is affecting the mid and lower tropospheric temperature significantly near the snow extent boundary. Namias then postulated that enhanced baroclinicity near the edge of the snow extent can lead to a positive reinforcement of the temperature contrast (and thus, baroclinicity) due to developing MLCs within this region. Namias (1978) cites a similar mechanism of enhanced baroclinicity near the east coast of the United States due to anomalous snow cover for the winter of 1976-1977.

Ross and Walsh (1986) found that snow cover near a coastal boundary plays a larger role in MLC trajectories than snow cover in inland areas. This finding is similar to what is seen in Namias (1962)'s work because the snow extent during his study approached the Gulf of Mexico and eastern coast of the United States. Ross and Walsh also found that inland snow played a role in MLC paths. However, it is not known how important this effect was overall because the study is limited to storms that had trajectories parallel to and within 500-600 km of the snow extent boundary.

The most recent study to consider the role snow cover plays on MLCs was Elguindi et al. (2005). Elguindi et al. modified snow cover under observed MLCs using a mesoscale

model (MM5) in the Great Plains. Using the Great Plains as the domain reduces the likelihood that land-ocean contrast is the primary mechanism influencing the MLC. Using two simulations, one with observed snow cover and one in which the entire model domain was snow covered, they found that there was little change to MLC trajectories. The MLCs in their simulations weakened because the snow cover removed a significant portion of the energy from the land surface. These findings were used to argue against Namias (1962)'s postulation. It is important to note that by filling the entire domain with snow, the MLC is no longer near the snow cover boundary that both Namias (1962) and Ross and Walsh (1986) postulated is necessary for a positive feedback mechanism. With the MLC significantly separated from the snow extent boundary, it is removed from the region of enhanced baroclinicity.

More frequent and widespread observations and advances in reanalysis products allow us to now take a closer look at the relationship between snow cover and MLCs. In this thesis, we will use the North American Regional Reanalysis (NARR) to (1) identity snow cover extent and MLCs and (2) assess the relationship between the two. The previous studies investigated the relationship between storms known to exist along the edge of the snow extent, but one question that remains is how common are MLCs near the snow extent edge? We will attempt to answer the following questions:

1. How well is the NARR able to represent snow cover extent and mid-latitude cyclone trajectories?

2. Is there a relationship between preexisting snow cover extent and mid-latitude cyclone trajectories?

3. Is there a region of enhanced baroclinicity near the snow extent edge?

Based on previous literature, we hypothesize that the snow extent boundary will be a preferential region for MLC centers due to increased low-level baroclinicity. The enhanced

low level-baroclinicity will mainly be driven by the enhanced temperature gradient across the snow-covered to bare-ground boundary due to differences in surface energy balance.

1.2 Snow-atmosphere Coupling

Snow cover has a large impact on the surface radiation budget due to the high albedo of snow compared to other surface types. Bauer and Dutton (1962) observed that snow cover resulted in the largest seasonal variation of surface albedo; based on magnitude of variability, there are essentially two surface albedo states–snow covered and not snow covered.

1.2.1 Local Response

The impact of snow cover was noted in assessing the forecast temperature bias of numerical weather prediction models (Dewey, 1977; Wojcik and Wilks, 1992); observational analysis then provided evidence of a relationship between snow cover and surface air temperature (Namias, 1985; Walsh et al., 1982; Namias, 1985). Baker et al. (1992) attributed a temperature depression of about 8°C for deep snow and about 6°C for intermediate snow depth as compared to no snow in Minnesota using station data. Ellis and Leathers (1998) attributed a 1-4°C depression using observations and a one-dimensional snowpack model. However, Cohen and Rind (1991) showed that a cooling effect would only last for a short time because the increased stability of boundary layer would lead to smaller latent and sensible heat fluxes, thus negating some of the cooling one would expect. Other studies have related the snow depth to the amount of cooling realized (Alexander and Gong, 2011; Dutra et al., 2011; Mote, 2008; Ellis and Leathers, 1999; Baker et al., 1992).

The short term temperature gradient induced by the snow to no snow boundary is great enough to create its own mesoscale circulation (e.g., Johnson et al., 1984; Taylor et al., 1998; Segal et al., 1991a). During solar heating, the bare ground warms much more

quickly than the snow-covered ground, leading to a circulation from the snow-covered ground to the bare ground. This effect has been termed a "snow breeze" (Johnson et al., 1984). The effect was first noted in Johnson et al. (1984) where they observed a region of snow-free ground surrounded by snow-covered ground. During the day, the snow-free region developed clouds that produced precipitation while the snow covered ground remained mostly cloudy. The finding was later observed in boreal forests (Taylor et al., 1998) and through aircraft observations in the Great Plains region (Segal et al., 1991a). Segal et al. (1991b) developed a mesoscale model with an interactive snowpack and found that the "snow breeze" is most likely to occur in spring due to the increasing incident solar radiation, which allows for stronger absorbed radiation gradients. A basic schematic of local response setup is shown in Figure 1.

1.2.2 Remote Response

Snow cover anomalies have been shown to excite remote responses at both the regional (e.g., the East Asian Monsoon in Zhang et al., 2004) and hemispheric scale (e.g., Walland and Simmonds, 1996; Cohen and Entekhabi, 2001). Walland and Simmonds (1996) ran simulations of climatologically high and low snow cover in the Northern Hemisphere without any seasonal variation. Snow cover anomalies between North America and Eurasia are shown to co-vary (Walland and Simmonds, 1997), so it is not unreasonable to run these simulations across the entire Northern Hemisphere. Walland and Simmonds (1996) find that increased snow cover in the Northern Hemisphere results in a decreased pole to equator temperature gradient in the North Atlantic and an increased temperature gradient in the North Pacific. This finding agrees with their MLC frequency counts that show diminished storm activity in the North Atlantic and increased storm activity in the North Pacific. Cohen and Entekhabi (2001) come to a similar conclusion using a seasonally varying global circulation model (GCM) experiment. Snow cover anomalies in

Eurasia are shown to be partly responsible for the quasi-biennial model of the Arctic and North Atlantic oscillations (Allen and Zender, 2011b,a), which are a measure of sea-level pressure variability. Variability in the sea-level pressure field is strongly related to cyclone activity in the region. It has been suggested that vertically propagating Rossby waves are the link from snow cover anomalies to the circulation response (Allen and Zender, 2011b; Fletcher et al., 2009). Eurasian snow cover anomalies not only have significant impacts during the winter, but also during the summer due to the increased duration of snow cover and amount of soil moisture (Matsumura et al., 2010; Matsumura and Yamazaki, 2012).

The impact of North American snow cover on Northern Hemispheric circulation has been studied less frequently than Eurasian snow cover. Eurasian snow cover extent is more likely to have an impact on Northern Hemispheric circulation because it is much more expansive than North American snow cover (twice as large during the winter (Walsh, 1984)). Recent work has shown that the effect of North American snow cover is not negligible (Leathers et al., 2002; Sobolowski et al., 2007; Klingaman et al., 2008). Leathers et al. (2002) showed that frequency of North American air mass types was influenced by snow cover extent. Upper atmosphere anomalies during the fall and late spring are supportive of the observed snow cover extent during those periods suggesting that it is the atmospheric circulation at upper levels driving the air mass frequency and snow cover extent. During the late winter and early spring the upper air anomaly pattern is weak and Leathers et al. (2002) hypothesize that snow cover will have a significant impact on air mass frequency during that period.

Sobolowski et al. (2007) hypothesized two possible ways modified air masses in North America can affect European climate: a stationary wave response and the alteration of the North Atlantic storm track. The former is a result of increasing the strength of the climatological high pressure over the North American continent during the winter, which

results in the entire climatological pattern shifting eastward in the northern hemisphere. The latter occurs due to changes in MLC trajectories from snow cover extent anomalies, much like Namias (1962) postulated. The results of Klingaman et al. (2008) suggest that (1) snow cover in the Great Plains adds positively to the North Atlantic Oscillation Index, influencing European climate and (2) that regional changes in snow cover have a larger impact than continental snow cover changes. Sobolowski et al. (2010) confirmed a transient eddy response to anomalous snow forcing and that the response was a result of enhanced baroclinicity in existing storm track entrance regions of the North Atlantic. It has been shown more recently that the largest driver of the stationary wave response is the cooling from increased snow cover and vice versa (Sobolowski et al., 2011).

1.3 Snow Cover Observing Techniques

Regular measurements of snow cover properties date back to the late 1800s and typically were based on the presence of snow cover or lack of snow cover (Brown and Armstrong, 2008). Station observations in the United States can be reliably traced back to 1900 with some caveats about data quality that make identifying trends difficult (Kunkel et al., 2007). Satellite observations were a large improvement over the point measurement interpolation techniques used before one could observe global snow cover directly (Matson and Wiesnet, 1981). The satellite era has allowed for global monitoring of snow cover and it is the longest running product produced from satellite observations, dating back to 1966 (Brown and Armstrong, 2008). Early satellite era observation techniques were manual interpretations of visible satellite imagery because of the unique albedo of snow compared to other land surface types. In some cases (e.g., Hall et al., 1995), multispectral instruments were used to aid in identifying snow cover by looking for a surface with a high albedo in the visible and a surface that is almost a blackbody in the infrared. All visible imaging techniques suffer when cloud cover obscures the view of the ground

(Brown and Armstrong, 2008) and visible sensing techniques do not provide any information on snow depth or snow water equivalent (SWE). Passive microwave observations can be used to overcome these limitations by penetrating clouds, operating without sunlight, and estimating snow depth (Brown and Armstrong, 2008). Chang et al. (1987) developed the first algorithm to estimate SWE because the amount of liquid water in the snowpack changes the ratio of certain microwave bands. Grody and Basist (1996) uses passive microwave observations to determine snow cover by looking for the ratio of scatter between high and low frequencies and then implementing other criteria to screen out precipitating clouds and frozen soil, both of which produce scatter ratios similar to snow cover. Active remote sensing (i.e. radar) from satellite platforms increases the spatial resolution of snow cover products, thus, they observe much less ground in a given time period (Nghiem, 2001).

1.4 Snow Cover Trends

With anthropogenic climate change (ACC) resulting in a mean global temperature rise, snow cover extent is expected to decrease because of its 0°C threshold dependence. Frei et al. (1999) find a general increase in snow cover extent during winter from 1930 to 1980 and then a decreasing trend in snow cover extent from 1980 to 1994. Similar results are seen in Brown (2000) with the most significant decrease in snow cover extent occurring during the spring. Snow cover extent exhibits the most autocorrelation during the spring and early summer (Déry and Brown, 2007) suggesting that snow cover can keep a "memory" of the winter in the system until mid-summer. Therefore, snow cover may play a role in atmospheric circulation during the spring due to its anomalous persistence. With the most observed change in snow cover extent as well as the most memory of snow cover on the climate system occurring in the spring, it is vitally important to understand how snow cover impacts atmospheric circulation. Brown and Mote (2009)'s analysis

of climate models from CMIP3 show that a continued reduction in snow cover extent through the year 2100 is likely, especially in coastal regions. However, where snow cover does remain, there will likely be an increase in the amount of snowfall due to increased precipitation (Brown and Mote, 2009).

1.5 Mid-latitude Cyclone Trajectories

It is important to make the distinction between a storm track and a storm trajectory. Generally, a storm track is a region of enhanced cyclone activity and a storm trajectory is the path of an individual MLC. A storm track is typically defined as a 2-7 day band-pass filter of geopotential height variance (Blackmon, 1976). This method isolates disturbances that cause variability in height in the order of 2-7 days and therefore is biased towards stronger disturbances. Storm tracks are more pronounced in the Northern Hemisphere during the winter at mid-latitudes and the spatial maximum occurs in both the North Atlantic and North Pacific (Chang et al., 2002). One might expect that transient eddies would remove existing baroclinicity in the region by transporting warm air northward and cool air southward decreasing the temperature gradient. Airmass movement in this manner would be detrimental to the existence of storm tracks (Hoskins and Valdes, 1990). A linear, stationary wave model in Hoskins and Valdes (1990) shows that baroclinicity generated by ocean heating off the east coast of continents acts to help maintain a storm track. The longitudinal extent of the storm tracks are thought to controlled by the eddies contained within the storm rather than continental effects (Kaspi and Schneider, 2011). A complete review of storm track dynamics is presented in Chang et al. (2002).

Another way to define the storm track is by frequency counts of MLCs. The frequency count method requires that individual MLCs be identified and tracked. Methods of identification and tracking are discussed briefly in 1.5.1 and 1.5.2, respectively. A comprehensive review on MLC identification, tracking, and frequencies is presented in

Ulbrich et al. (2009). There are two common ways to do frequency counts. The first method is to count MLC occurrence at each grid point within the domain. This method is biased towards slow-moving storms because it assumes that a storm will not skip a grid point. A fast-moving storm may pass over a few grid points between each time step and therefore it will not be counted at those grid cells. The second method is to count MLC occurrence within a certain distance of each grid point. This method will be biased towards fast-moving storms because a single storm can be counted in more grid boxes in a shorter period of time.

1.5.1 Identification

Numerous subjective and objective MLC identification methods have been developed. Early methods required researchers to manually analyze weather maps (e.g., Klein, 1957). However, hand analysis is tedious, time consuming, and prone to human error. Different forecasters may interpret a particular weather situation differently (Haak and Ulbrich, 1996) resulting in different MLC climatologies due to their subjective location (or lack thereof). To overcome the inherent issues with subjective MLC analysis, automated methods have been developed.

The most common automated MLC detection methods are minima location detection methods. Typical fields for analysis are mean sea-level pressure (e.g., Lambert, 1988; Murray and Simmonds, 1991; Chandler and Jonas, 1999; Lionello et al., 2002; Bauer and Del Genio, 2006) and 1000 mb height (e.g., Alpert et al., 1990; König et al., 1993; Blender et al., 1997). One issue with the minima methods is that centers are often reported as the grid cell where the minimum is observed, neglecting the fact that coarse grids may not be able to accurately represent the true center of a MLC. Murray and Simmonds (1991) fit a complex function to the mean sea-level pressure field to better identify the true center of MLCs. A second issue with the minima method is the conversion of surface

pressure to mean sea-level pressure. Studies have excluded regions of high topography due to this issue (Ulbrich et al., 2009). Minima finding methods will be biased towards more developed MLCs because they require a well-defined pressure or height field while some studies (e.g., Blender et al., 1997; Gulev et al., 2001) require a minimum pressure or height depression. The number of MLCs identified using minima finding methods is highly dependent on the spatial resolution of the dataset (Blender and Schubert, 2000). Low spatial and temporal resolution models are more likely to miss weaker MLCs (during genesis or decay phases) than higher resolution models because the scale of the features may be smaller than the grid scale or have a duration shorter than a time step (Blender and Schubert, 2000).

A second identification method is to identify vorticity maxima (e.g., Hodges, 1994; Sinclair, 1997). Identifying vorticity has a few advantages over mean sea-level pressure or 1000 mb height identification. The biggest advantage to the vorticity method is that it helps remove the well developed storm bias by identifying faster and weaker MLCs (Sinclair, 1997). Typically, the vorticity signature is more pronounced for small MLCs where a mean sea-level pressure minimum may not even be present (Hodges et al., 2003).

Numerous other identification methods have been studied in recent years. Hoskins and Hodges (2002) reviews identification methods ranging from those best suited for small scales (vorticity and potential vorticity), medium scales (meridional wind, temperature, vertical velocity), and large scales (mean sea-level pressure and geopotential height). BENESTAD and CHEN (2006) develops a calculus-based identification method by finding Fourier approximation coefficients and then solving for minima in the decomposed mean sea-level pressure field using a derivative technique. Hewson and Titley (2010) incorporates frontal detection into a combined vorticity maxima and mean sea-level pressure minima scheme. Hewson and Titley's scheme makes significant improvements identifying and tracking at high spatial resolutions. While not explicitly used to

identify MLCs, a clustering technique using regression of the circulation to the environment developed in Cannon (2012) may allow identification of MLCs based off of several characteristics of MLCs (e.g. sea level pressure, temperature).

1.5.2 Tracking

After identifying MLCs at each time step it is often necessary to link MLCs at subsequent time steps. Most tracking methods follow some variation of the nearest-neighbor approach (e.g., Murray and Simmonds, 1991; Chandler and Jonas, 1999; Lionello et al., 2002) that finds the closest MLC center at the next time step. Forecast values of MLC centers are sometimes used to aid in MLC tracking. For example, Murray and Simmonds (1991) use MLC velocity history to estimate future locations, Chandler and Jonas (1999) imposes criteria on the maximum speed and requires that the storm generally move eastward, and Lionello et al. (2002) creates a box around a MLC center that is based on the current size of the MLC.

The main issue with the nearest-neighbor approach is that at time steps of 12 hrs or greater the theoretical distance a MLC can move is similar to the typical spatial separation of the MLCs at any particular time step (Murray and Simmonds, 1991). Therefore, the shorter the time between MLC identifications the easier it is to relate MLC centers. The separation issue was more significant in early numerical weather prediction models where model output was 12 hrs or greater. With advances in computing resources, temporal output has decreased to 3-6 hrs or even less. However, with increasing temporal resolution, the amount of computing time and resources needed for identifying MLCs increases.

Many studies require a minimum track length in their detection algorithm (e.g., Chandler and Jonas, 1999; Hodges et al., 2003) in order to remove weaker storms. Typical minimum track lengths range from 12 hrs (Wang et al., 2006) to 36 hrs (Chandler and

Jonas, 1999). As seen with requiring a minimum depression in either mean sea-level pressure or 1000 mb heights, requiring a minimum track length to remove spurious MLC centers will again increase the bias toward more well developed MLCs. Grigoriev et al. (2000) provides an automated interface for manual tracking. After automated identification of MLCs, a user-friendly interface is provided so that a user can easily click and relate centers together into a track. This allows for more logical path connection and termination based on the meteorological situation than what can be done via current automated algorithms, but the method also introduces subjectivity to the algorithm. Inatsu (2009) developed a tracking algorithm that can handle merging and separating MLCs.

1.6 Mid-latitude Cyclone Trends

Recent reanalysis data suggest a decrease in MLC frequency over time and a shift poleward. Gulev et al. (2001) find a statistically significant reduction of -12 MLCs per decade, but an increase in MLCs that exhibit a central pressure below 980 mb. The trend at higher latitudes is smaller (-0.2 MLCs per decade) and not statistically significant as compared to the entire Northern Hemisphere. A similar negative trend is seen in Wang et al. (2006) for the North Atlantic, but the trend for only MLCs at northern latitudes is shown to be positive. The previous findings are in agreement with Sickmoller et al. (2000) who also identify a reduction in the number of MLCs and a poleward shift in the remaining MLCs. The results of Wang et al. (2006) also suggest a poleward shift and quantify the change as 181 km between 1958 and 2001. Gulev et al. (2001)'s finding of an intensification of MLCs was shown to be more significant using principle component analysis by Geng and Sugi (2001). Reanalysis and observations suggest that over approximately the last 50 years MLCs have decreased in number, shifted poleward, and become more intense (IPCC, 2007).

Similar findings have been seen in general with GCM experiments forced by ACC, suggesting that the observed trends will continue. However, the results are not as coherent as the trends from reanalysis. Bengtsson et al. (2006), using the ECHAM5 model, finds a poleward shift of storm tracks, but that there is no change in the intensity of the MLCs. CCSM3 model results show a decrease in MLC frequency, no visible poleward shift, and any changes in intensity are confined to certain geographical regions (i.e. North Pacific) (Finnis et al., 2007). Long et al. (2009), using the Canadian Climate Centre model with a regional model (Canadian Regional Climate Model) for downscaling the western North Atlantic, find an 11% reduction in MLC frequency and no statistically significant change in storm track location within their domain. Using a different regional mesoscale model (Canadian Mesoscale Compressible Community) over approximately the same domain for the fall (as compared to winter for Long et al. (2009)), Jiang and Perrie (2007) shows a statistically significant shift in the storm track poleward. There is more uncertainty with changes under ACC, but the emerging consensus is for a continued trend of what has been observed over the last few decades. It is still uncertain why there is a poleward shift in storm tracks.

In this thesis, we have chosen the best practices from the aforementioned papers to investigate the role snow cover has on MLCs. A simple MLC identification and tracking scheme based on mean sea-level pressure was chosen because it is fast to run at high spatial and temporal resolution and provides the right balance of storm intensities. Previous research has demonstrated that there is considerable evidence for a link between snow-covered ground and the atmosphere at various scales.

2 Data and Methods

A high temporal and spatial resolution analysis is needed in order to understand the synoptic and mesoscale processes that are involved in land-atmosphere coupling because MLC identification and tracking is sensitive to temporal and spatial resolution (Blender and Schubert, 2000). In order to meet these requirements and to maintain a physically consistent relationship between snow on the ground and the atmosphere, the North American Regional Reanalysis (NARR) was used. In this section we describe the datasets (NARR, Snow Data Assimilation System, and Atlas of Extratropical Cyclones) and methods (Snow cover extent, MLC identification, MLC tracking, and low-level baroclinicity) we will use to investigate the relationship between MLC trajectories and snow cover extent.

2.1 North American Regional Reanalysis (NARR)

The NARR is a high spatial and temporal resolution reanalysis dataset for North America from 1979-present (Mesinger et al., 2006). NARR has a horizontal grid spacing of approximately 32 km and consists of 47 layers in the vertical. NARR snow depth (snod) and pressure at mean sea-level (prmsl) netCDF files were obtained from the website of NOAA/OAR/ESRL PSD, Boulder, Colorado, USA, at `http://www.esrl.noaa.gov/psd/`.

NARR uses the Noah land surface model to simulate the snowpack. The snow-water equivalent base state is updated at 0000 UTC using the United States Air Force snow depth from their SNODEP model (Mesinger et al., 2006). SNODEP is run daily at 1330 UTC and uses a combination of station data, satellite retrievals, and manual interpretation to produce snow depth, snow age, and ice cover over water on a 48 km grid (Kopp and Kiess, 1996). Linear inverse weighting, using the nearest five grid points, is used to determine the snow depth at a grid point (subject to spatial homogeneity

checks). If there are no other grid points within 250 km of a grid point, then a satellite remote sensing algorithm (Special Sensor Microwave Imager) is applied to determine snow depth. Satellite retrievals cannot remove snow from any grid points already determined to have snow. Manual modification of snow depth is performed at times (Kopp and Kiess, 1996). However, manual modification typically only occurs over large regions and not individual stations. In addition, manual modification is not done for every day or for all regions. SNODEP has issues with complex topography (Kopp and Kiess, 1996).

2.2 Snow Cover Extent

Snow cover extent was objectively determined from NARR snow depth using a simple algorithm that located the latitude of continuous snow cover across North America. For a given day, the snow extent was analyzed at 0000 UTC. The analysis was only performed at this time because NARR tends to exhibit an unrealistic variation in snow cover throughout the day (National Centers for Environmental Prediction, 2007). At 0000 UTC, NARR should be closest to truth because that is when the estimated snow cover from SNODEP is assimilated. The snow depth was converted to a categorical snow cover and linearly interpolated to a 0.25° grid spanning 130° W to 62° W and 10° N to 80° N.

Grid points that have snow at some location in each cardinal direction are set to be covered. This is done to account for one of two possible cases, the first of which is to remove noisy data. At times, the snow cover map contains areas that are not covered, even though they likely are based on the synoptic snow cover pattern. The second case is to aid in determining the relevant extent of the snow cover. In a situation where a storm deposits snow significantly far away from the existing extent, a swatch of non snow-covered ground may appear between the new snow and old snow. For the purpose of this study we are interested in the southern extent of the snow and the algorithm may

not sense it as continuous if the swath of no snow is present.

The algorithm searches each longitude bin, from south to north, looking for ten consecutive snow covered points (equal to 2.5°). When ten consecutive snow covered points are found the snow extent is set to the first (most southern) point in the snow covered region. After finding the latitude of snow cover extent at each longitude bin the line is smoothed by running a ten point filter forward and backward to prevent phase shifting. A sample identification of snow cover extent is shown in Figure 2.

2.3 Mid-latitude Cyclone Trajectories

MLC trajectories were identified by finding a local minimum in NARR sea-level pressure and tracking it at subsequent time steps. The sea-level pressure field at each time step was linearly interpolated to two grids with spacing of 0.25° (fine) and 2.5° (coarse). The interpolated grids cover the region from 155° W to 60° W and 20° N to 65° N in order to allow adequate space from the domain edges for the local minimum finding to be reliable. Critical points were found at both grid spacings by taking derivatives in the north-south and east-west orientations and then finding the intersection of the zero derivative contours. Minima, maxima, and saddle points are differentiated by the second derivative in both orientations at the critical points. The minima are then set to be at the closest grid point. The coarse resolution identifications were then refined by changing their location to the nearest fine resolution minimum. Relating the coarse resolution to the fine resolution is done to improve the accuracy of the coarse resolution and to ignore the noise in the fine resolution. The fine resolution identifies nearly 10 times the amount of pressure minimum as the coarse resolution (Figure 3).

Tracking is performed using a nearest-neighbor method to link pressure minimum together into coherent storms over time. At every time step, all the pressure minima are attempted to be related to a pressure minimum at the next time step. At subsequent

3 hourly time step steps, storms are searched for within a radius of 361 km (3.25° on a sphere of radius 6371 km measured along a great circle) of the current storm position. A search radius of 361 km equates to a cyclone speed of approximately 120 km hr^{-1}. The speed is similar to the 100 km hr^{-1} used in Blender and Schubert (2000) and is the same as the 120 km hr^{-1} used in studies based off the work of Chandler and Jonas (1999). The nearest pressure minimum, within the search radius, is set to be part of the same storm as the previous minimum. To prevent pressure minimum from unrealistically backtracking, future pressure minimum must be located in a region generally to the east of the previous location. The region is defined as being between compass angle 355° and 185°. Pressure minimum identified as being part of a storm are not used in future searches. In the case when no pressure minimum is found within the search radius, the search radius is doubled and the six hour pressure field is searched. If a pressure minimum is found within the search radius, then it is set to be part of the storm with the current point. If a pressure minimum is not found at the plus six hour time step, then the storm ends. If in any six hour period a storm has not moved more than 0.25°, then the track is terminated. The process continues for every pressure minimum in the entire dataset. The tracking creates a storm database that contains the latitude, longitude, pressure, date, and time of the storm center at each three hour time step of the MLC.

2.4 Comparison of NARR to Other Products

In order to build confidence in our choice to use NARR, we compare our snow cover extent and MLC trajectories to other datasets. The snow cover extent algorithm is applied to both NARR snow cover and the Snow Data Assimilation System (SNODAS) and results compared. The storm trajectories identified in NARR are evaluated qualitatively against the Atlas of Extratropial Storm Tracks from Chandler and Jonas (1999).

2.4.1 Snow Data Assimilation System (SNODAS)

SNODAS is a modeling and data assimilation framework to estimate snow cover and related variables (Barrett, 2003). SNODAS, along with other snow and ice data, can be downloaded at `http://nsidc.org/data/`. SNODAS incorporates (1) quality controlled and downscaled numerical weather prediction output, (2) a snow pack model, and (3) a data assimilation scheme (Barrett, 2003). The data assimilation scheme takes observations from satellite, airborne instruments, and surface observations. The dataset has 1 hr temporal resolution and 1 km horizontal grid spacing. It is difficult to assess the quality of SNODAS because there is no other dataset of snow cover with similar temporal and spatial resolution (Barrett, 2003). The quality of the final product depends on the number and quality of observations used; if there are no observations within a region (such as, a lack of surface stations or cloud cover obstructing the view from satellites), then SNODAS output is solely model output (Barrett, 2003).

2.4.2 Atlas of Extratropical Storm Tracks

The Atlas of Extratropical Storm Tracks is a product of Chandler and Jonas (1999) at the Goddard Institute for Space Studies. The database contains global extratropical storm trajectories for storms lasting at least 36 hrs for 1961-1998. The extratropical cyclones (hereafter referred to as MLCs) are identified as minima in the mean sea-level pressure field from 12 hr temporal and 2.5° spatial output of the NCEP Reanalysis project (Chandler and Jonas, 1999). Storms within 1440 km of one another at subsequent time steps are joined together as long as they do not form an acute angle of less than 85° over the 12 hr period (Chandler and Jonas, 1999). As seen from the discussion in Section 1.5.1 and Section 1.5.2, Chandler and Jonas (1999) will favor well-developed storms because of (1) low spatial resolution (2.5°), (2) requiring MLCs to last for at least 36 hrs, and (3) using sea-level pressure (as compared to vorticity tracking).

2.5 Low-level Baroclinicity

The commonly suggested mechanism for why there should be a relationship between snow cover extent and MLC tracks is that there is a region of enhanced low-level baroclinicity near the snow cover extent. To investigate this, a measure of low-level baroclinicity is developed for NARR. A measure of baroclinic instability is (Lindzen and Farrell, 1980; Hoskins and Valdes, 1990):

$$\sigma_{BI} = 0.31 \times \frac{f}{N}\frac{d\mathbf{v}}{dz} \tag{1}$$

where f is the Coriolis parameter, N is the Brunt-Väisälä frequency, $\mathbf{v}$ is the horizontal wind, and z is height. The Brunt-Väisälä frequency and Coriolis parameter are defined as

$$N = \sqrt{\frac{g}{\theta}\frac{d\theta}{dz}} \tag{2}$$

$$f = 2\Omega \sin\phi \tag{3}$$

where θ is potential temperature, g is gravity, Ω is Earth's angular speed, and ϕ is latitude. The metric σ_{BI} is a measure of the growth rate of a baroclinic wave and is sometimes referred to as the eddy growth rate (Long et al., 2009). The larger the values of σ_{BI}, the faster a disturbance will grow. Therefore, it is a good proxy for where storms will preferentially develop.

To use this equation as a measure of low-level baroclinicity in NARR a few modifications need to be made. NARR output is on pressure levels and therefore pressure levels may intersect the ground. Pressure levels intersecting the ground make it difficult to calculate low-level baroclinicity at a constant height above the surface. To overcome this issue, pressure at the surface for each grid point was used to define what the maxi-

mum pressure value was in a column. Then, the first pressure level that is 150mb lower than the surface pressure is set to be the lower altitude pressure level. The pressure level higher in altitude is set to be the middle. The middle level is where the low-level baroclinicity is estimated. The upper level for the finite difference approximation is set to be the level that is two levels above the lower level.

The modifications allow us to express the low-level baroclinicity in NARR with the following equation:

$$\sigma_{BI} = 0.31 \times \frac{f}{\sqrt{\frac{g}{\Theta_m}\frac{\Theta_u - \Theta_l}{\Phi_u - \Phi_l}}} \left| \frac{V_u - V_l}{\Phi_u - \Phi_l} \right| \tag{4}$$

where σ_{BI} is a measure of the low-level baroclinic growth rate, f is the Coriolis parameter, g is gravity, $\Theta_{l,m,u}$ is the potential temperature at the lower, middle, and upper level, $\Phi_{l,m,u}$ is the geopotential height at the lower, middle, and upper level, and $V_{l,u}$ is the magnitude of the wind at the lower and upper level. The eddy growth rate is then linearly interpolated to the 0.25° spacing use for all the other calculations and analysis.

Using the aforementioned process, low-level baroclinicity is typically calculated at a pressure level ranging from 800 mb over low topography and up to 550 mb in high topography. The typical bottom layer for the discretization is just above the boundary layer at approximately 155-190mb above the surface ($\sim$ 1-2 km). The layers on which low-level baroclinicity are calculated remain relatively constant throughout the year and rarely vary by more than two model pressure levels. A sample day of low-level baroclinicty is shown in Figure 4 along with the pressure level where the calculation is valid.

2.6 Statistical Analysis

To answer the question of whether there is a relationship between snow cover extent and MLC trajectories the distance from the snow extent line to the MLC center is studied. The distance from the MLC center to the nearest snow cover extent point is calculated

using the snow cover and MLC position on the same day (zero lag). Typically, the distance calculated is north to south, but in some instances, such as near the Rocky Mountains, the shortest distance may be east to west oriented. If the MLC center is over snow, then the distance value is set to be negative. If the MLC is not over snow, then the distance is set to be positive. This means that negative distances are found north of the snow extent line, while positive values are found south of the snow extent line.

The distance was calculated for all months, except for June through September, which were removed. During the summer and early fall, the snow extent approaches the northern edge of our domain. We do not have confidence in the results when the snow extent is near the edge of our domain due to the inability of our algorithm and model to simulate snow cover in that region. The results will be discussed with relation to three seasons, the fall, the winter, and the spring. November is presented as the representative member of the fall (October and November), January as the winter (December, January, February), and March as the spring (March, April, May). The fall and spring are sometimes referred to as the shoulder seasons.

To investigate the significance of the enhanced peaks, distributions of the distances using shuffled snow cover extent were calculated. The resulting distributions were then subtracted from the distribution using snow cover and MLC centers in the same year. Summing the differences between all the distributions shows where the most consistent change is occurring. It is assumed that shuffling the data will create mostly random noise that will cancel when summed. Any non-random noise will result in peaks.

3 Results

The following section provides general statistics and evaluation of our NARR-derived snow cover extent and MLC climatology. The relationship between MLC centers and snow cover extent is investigated and the robustness of the relation is evaluated. Low-level baroclinicity is studied to determine its role in any coupling between snow cover and MLCs. Unless otherwise noted, the following analysis was performed for 0000 UTC 01 January 1978 to 2100 UTC 31 December 2010.

3.1 Snow Cover Statistics

Mean latitude of snow cover extent for each day between 125° W and 67° W was calculated. Snow cover extent features a large mean annual cycle ranging from its most southern extent at 40.2° N in January to its northern most extent in August at 70.1° N. Mean monthly snow cover extent experiences its largest variability during the spring and the fall. The most southern monthly mean snow extent occurred in January 1979 at 38.0° N. The single day maximum snow cover extent occurred on February 5th, 1996 when mean longitudinal snow cover extent was 35.4° N.

There is no clear trend in mean monthly latitude of snow cover from 1979-2010 (Figure 5). Two months (May and December) have a negative slope, which suggests that mean monthly snow cover extent has shifted farther south. The remaining months all have positive slopes signaling that snow cover has retreated farther north. The only statistically significant trends at the 95% confidence level occur in May ($p = 0.02$), October ($p = 0.0005$), and November ($p = 0.02$). Relaxing confidence to the 90% level does not add any months.

3.2 Snow Cover Extent Evaluation

Our algorithm for snow cover extent was also applied to the SNODAS dataset for 2004 to 2009. The root mean square error (RMSE) between NARR and SNODAS snow cover extent for each degree longitude from October to May is 4.5°. Figure 6 shows frequency distributions of the difference between NARR and SNODAS. In general, NARR tends to be farther north than SNODAS. The mean of difference for each longitude (Figure 6a) is better than the difference in the mean latitudinal extent across all longitude points (Figure 6b). The winter typically agrees within -0.3° to 1.7° latitude when comparing each point and the difference of the mean latitude of snow cover extent increases to 0.7° to 2.6°. Almost all of the differences greater than 10° occur over mountain ranges. The largest differences appear in the Rocky Mountains and slightly less frequent large differences appear in the Sierra Nevada mountain range. Small peaks of large differences are also seen over the Appalachian Mountains, but not nearly as frequently as other mountain ranges. Differences greater than 5° exhibit a similar relationship in mountain ranges. Excluding mountainous areas, the two datasets typically agree within 5° latitude with NARR tending to have a northern bias as compared to SNODAS.

Summary statistics of our algorithm applied to six years of SNODAS are similar to 32 years of NARR. The maximum monthly mean snow cover extent shifts from January to February and shifts further south to 39.0° N from the 40.2° N in January in NARR. The separation between mean monthly snow cover extent between January and February is smaller for SNODAS (0.1° N) than for NARR (0.5° N). The mean snow extent retreat from March to May occurs much more slowly in SNODAS (0.9° per month) than NARR (3.6° per month).

3.3 Cyclone Statistics

The following statistics apply to the region between 125° W and 67° W and 20 ° S to 65° N. It is important to note that storms can both enter and leave our domain because of the inherent nature of a regional reanalysis product. Therefore, we cannot make any statements on genesis or the true duration of storms. The statistics provided in this section are only valid for our region of interest.

The average number of MLCs identified by our algorithm was 1644 per year. The maximum number of MLCs occurred in 2004 with 1822 identified and the minimum occurred in 2010 with 1568. The maximum number of storms happened during the summer and the minimum number of storms occurred during the winter. The reversal from conventional thinking about the frequency of MLC between the summer and winter is a result of our limited domain and tracking algorithm. The average duration of identified MLCs is 23.1 hrs with a maximum average duration of 24.8 hrs in February and a minimum average duration in July at 20.8 hrs.

Constraining the results by increasing the minimum MLC duration to at least one day results in an average of 306 per year, a 81.3% reduction. Thus, a majority of our storms are tracked for a period of nine to twenty-four hours. The maximum number of storms (333) longer than a day occurred in 1984 and the minimum (277) was observed in 1980. Requiring longer duration storms shifts the most frequent period of cyclone activity to the spring (28.2 MLC per month). The summer becomes the month with the least amount of MLCs at 23.4 per month. The average length of MLCs increases to 50.0 hrs and there is little intermonthly variability (standard deviation of 1.1 hrs).

Increasing the minimum duration to at least 48 hrs (for comparison with other tracking methods that relied on 12 hr time steps) results in a 79.7% reduction to an average of 62.2 storms per year. The average storm duration further increased to 72 hrs and again there was little variation between months (standard deviation of 1.9 hrs). The

longest observed MLC within our domain was in May 1993, lasting for 165hrs (6 days and 21 hrs).

3.4 Mid-latitude Cyclone Trajectory Evaluation

Our database of MLC trajectories was compared visually to the Atlas of Extratropical storm tracks. Maps of storm trajectories from NARR were plotted over the storms from the Atlas of Extratropical Storm Tracks (Chandler and Jonas, 1999) for all months. Storm trajectories from NARR overlapped a majority of the storm tracks from Chandler and Jonas (1999). In some cases, the trajectories from Chandler and Jonas (1999) were represented by two different storms in our NARR database. As expected, due to differences in selection criteria and resolution, many more storm trajectories were identified in our NARR database than in the Atlas of Extratropical Storm Tracks. There are some instances where our algorithm does not identify a trajectory, but the Atlas of Extratropical Storm Tracks does. Without further investigation, it is unclear if it is missed in our database or mis-identified by their algorithm.

3.5 Relationship

First, we take a look at storms that last at least 24 hours in order to remove the weakest MLCs in our database. Analysis of storms shorter than a day will be presented later. Figure 7a is the histogram of the distance between the snow extent and the MLC centers for the month of November. The center of the distribution appears to be related to the snow extent line (zero distance). The maximum frequency occurs just south of the snow extent line and exhibits a longer tail south of the snow extent than to the north. The spring has a distribution that is very similar to the fall (Figure 7c). The main difference in March is a more pronounced peak in frequency just south of the snow extent line. The enhanced peak in frequency is from about 50-350 km south of the snow extent line.

The tail south of the snow extent line is not as large as November, but the frequency north of the snow extent line retains its shape with only a small increase in magnitude. The winter displays a similar characteristic to the shoulder seasons with one marked difference–January (Figure 7b). January has a bimodal distribution with a peak near the snow extent line and another peak approximately 450-750 km north of the snow extent line. Possible explanations for the peak north of the snow extent are presented in the discussion. The common trait among all months is an enhanced frequency of MLCs in a region 50-350 km south of the snow extent line.

There is approximately a 35% reduction in the number of MLC centers and 25% reduction in the number of MLCs when requiring storms to last at least 48 hours as compared to 24 hours. The distance between the MLC center and the snow cover extent in the fall does not have as pronounced peak as seen in storms lasting longer than a day (Figure 8a), despite 199 storms that are overlapped between the two time periods. The same is true for the winter with no enhanced peaks and, in addition, the distributions are centered around a region approximately 500 km north of the snow extent (Figure 8b). The spring season still exhibits an enhancement of MLC center frequency in a region of 50-350 km south of the snow extent line (Figure 8c). April and May exhibit stronger peaks than March.

Taking a broader look, storms lasting longer than nine hours are analyzed. Nine hours is the theoretical minimum time that produces reliable tracking from our MLC tracking algorithm. In the fall, there is enhanced frequency of MLC centers near the snow extent line in a region 0-200 km south of the snow extent (Figure 9a). This region is slightly farther north than storms lasting longer than one day. The distribution shows a higher frequency of MLC centers south of the snow extent and the frequency does not decay as rapidly as compared to storms lasting longer than a day. The winter distributions are very similar to their 24 hr counterparts. There is a bimodal distribution with one peak

in a region 100-300 km south of the snow extent and another peak in a region 600-800 km north of the snow extent (Figure 9b). Spring continues to show an enhanced peak 100-300 km south of the snow extent line (Figure 9c) as it has for all three time criteria. However, the drop in frequency south of the enhanced region is not as steep as the longer duration storms.

For an overview of the statistics for all months and subjective analysis of the distributions please refer to Table 1. Comparing the Atlas of Extratropical Storm Tracks (Chandler and Jonas, 1999) to snow cover extent instead of using our identified trajectories from NARR results in similar-looking distributions (not shown). For the remainder of the analysis, we focus on storms that last longer than a day because they exhibit the strongest relationship between the snow cover extent and the location of the MLC center.

3.6 Lagged Relationship

It can be argued that one would expect a relationship between mid-latitude cyclone tracks and snow cover extent because during the cold season it is generally anticipated that snow would be produced on the northern side of MLCs. Therefore, one may expect to see MLCs track just south of the snow extent when using no lag time. To investigate if this is an issue, lagged relationships were looked at with both snow cover extent and mid-latitude cyclone leading.

The results suggest that it is pre-existing snow cover that is related to the mid-latitude cyclone tracks and this is shown in Figure 10 , 11, and 12. The middle portion of each Figure is the distribution for a zero day lag with storms lasting longer than one day. The top portion is for a two day lag with snow cover leading the MLC and the bottom portion is for a two day lag with the MLC leading. A two day lag with snow cover leading is representative of snow cover leading for lags one to five. There is very little difference between the zero day lag and the other lag times with snow leading. With the snow

cover leading the MLCs there is still an enhanced frequency of MLC centers in a region approximately 50-350 km south of the snow extent line. There is a small shift to left observed in a few months. A strong leftward shift is seen with MLCs leading the snow cover extent by two days. The peaks with MLCs leading also tend to be larger, more pronounced, and nearly centered on zero distance.

3.7 Robustness

Comparing the distribution for the actual year to all other years shows the largest and most coherent structures in a region just south of the snow extent line (Figure 13). There are substantial differences in the distributions just south of the snow extent line when using snow cover extent from all other years. There is increased frequency of mid-latitude cyclone centers in a region 50-350 km south of the extent line when the snow cover extent and MLCs are from the same year.

3.8 Low-level Baroclinicity

Normalized mean low-level baroclinicity in 100 km bins surrounding the snow extent are presented in Figure 14. It is evident that baroclinicity peaks in a region just south of the snow extent in all months. The structure of baroclinicity is almost identical for all months with the smallest values in a region south of approximately 1500 km south of the snow extent and the largest values occurring in a region from the snow extent to approximately 1000 km south of the snow extent. The fall (Figure 14a) has a stronger peak than the other months because of much lower baroclinicity values north of the snow extent as compared to the winter and spring. The results show that the largest values of low-level baroclinicity occur in a region that roughly coincides with the peaks in MLC frequency. It is important to note that the enhancement of baroclinicity is much broader and not as pronounced at the MLC distance distribution peaks.

3.9 Variables Relative to Snow Cover Extent

Plots of select variables (albedo, temperature, latent heat flux, and sensible heat flux) relative to the snow cover extent are shown in Figure 15 for the month of March. The values represent composite mean daily values for each variable following the snow cover extent on each day. There is clearly a difference in albedo across the snow extent boundary (Figure 15a) with values north of the snow extent averaging between 35% to 55% and values south of the snow extent in the 15% to 25% range. The smaller scale structures in the albedo are tied to mountains and vegetation. The expected temperature structure relative to the snow extent is seen and shown in Figure 15b. There is a small enhancement of temperature gradient near the snow cover extent. Snow cover tends to mute the sensible (Figure 15c) and latent heat (Figure 15d) fluxes as compared to bare ground and they exhibit a structure that is related to the snow cover extent edge. The difference in sensible and latent heat fluxes is setting up a temperature anomaly pattern that is supportive of baroclinic instability.

4 Discussion

The results show that there is an enhanced frequency of MLCs in a region 50-350 km south of the snow extent. The region of enhanced MLC frequency is also the region where the largest values of low-level baroclinicity are experienced. In this section we will first discuss how valid our choice of using NARR is and then explain the features of the relationship between MLCs and snow cover extent. We will close with a postulation that snow cover extent may play a role in the northward shift of storm tracks seen under conditions of ACC.

4.1 NARR Evaluation

NARR snow cover extent and SNODAS snow cover extent compare well when using our snow cover identification algorithm (RMSE of 4.5°). Almost all of the large errors (≥ 5) occur in mountainous regions and it is likely that those regions dominate the RMSE. For example, restricting the snow cover extent evaluation to 95° W to 80° W (approximately the area east of the Rocky Mountains and west of the Appalachian Mountains) reduces the RMSE to 1.6°. The large errors in mountainous regions may be explained by the grid spacing of the datasets, despite linearly interpolating both datasets to a 0.25° grid. The quality of the interpolation will depend on the native spatial resolution. SNODAS is linearly interpolated from 1 km grid spacing to 0.25° ($\sim 27\ km$) and NARR is linearly interpolated from 32 km. Due to a higher spatial resolution, SNODAS is expected to better represent complex topography and therefore give a better representation of snow cover in mountainous regions. A better representation of complex topography also explains why there is a southern bias of SNODAS compared to NARR because our algorithm for the southern edge of snow cover extent is sensitive to high topography where snow tends to last longer than surrounding regions.

Trends in 1979-2010 North American snow cover extent are inconclusive because some

months (i.e. May and December) show an increase (more southern mean snow extent) and the other months show a decrease (more northern mean snow extent). A majority of the trends are not statistically significant. The statistically significant increase in snow cover extent during May is interesting because it is opposite result of the strong negative trends seen in Frei et al. (1999) and Brown (2000). The reason for the discrepancy may be explained by our algorithm because of how it acts in mountainous regions where snow remains for extended periods of time at high elevations. The algorithm may sense continuous snow cover in the mountains, but the continental snow cover pattern may suggest that the snow extent is actually much further north. With ACC in mountainous regions, SWE is expected to increase due to increased precipitation because they will still remain below the 0°C threshold (Brown and Mote, 2009). Regions with lower elevation will be more sensitive to AAC because their mean temperatures are closer to the 0°C threshold (Brown and Mote, 2009). Therefore, we expect the continental scale snow cover to continue to decrease due to rising temperature, but snow at high elevations to increase. The trend will result in our algorithm increasingly over estimating snow cover extent. Thus, our algorithm cannot reliably produce trends in snow cover extent due to inherent biases in mountainous terrain. However, our analysis of snow cover extent to MLC positions is still valid because the mountainous regions, where the issue is evident, are a small fraction of our domain. In addition, a similar relationship is seen when restricting the domain to be east of the Rocky Mountains and west of the Appalachian Mountains.

Visual comparison shows that our storm database contained most of the storm trajectories identified in the Atalas of Extratropical Storm Tracks (Chandler and Jonas, 1999). It is difficult to make a direct comparison between our database and other databases because of (1) differences in temporal and spatial resolutions, (2) different reanalysis datasets, and (3) lack of absolute "truth" with which to compare. Each method and

dataset is tailored to the specific needs of the question being asked. However, we have confidence that our database is adequate for our needs because the same relationship between MLC centers and snow cover extent is seen using both our database and the Atlas of Extratropical Storm Tracks, despite the differences in technique and large differences in temporal and spatial resolution.

4.2 Relationship Between Snow Cover and MLCs

There is a strong and robust relationship of the distance between MLC centers and the southern edge of the snow cover extent. The frequency distribution of MLC centers typically features enhanced peaks in a region south of the snow extent for storms lasting longer than one day and all the distributions are nearly centered near the snow extent line. A preferential region for MLC trajectories near the snow extent boundary supports the ideas postulated in Namias (1962) and Ross and Walsh (1986). From the aforementioned results, the region can be quantified as being 50-350 km south of the snow extent.

The bimodal distributions seen in a few months (mainly January) can plausibly be explained by Alberta Clippers. Alberta clippers are fast moving MLCs that are most commonly found in December and January (Thomas and Martin, 2007). Alberta clippers are generated in the lee of the Rocky Mountains in Alberta, Canada and generally track east-southeast toward the north central border of the United States where they then continue to progress eastward (Thomas and Martin, 2007). The trajectory of an average Alberta clipper is approximately 600 km to 800 km north of the mean January snow extent ($\sim$40° N). This region corresponds to the location of the bimodal peak observed north of the snow over extent in January. The fast-moving nature of these storms is the reason the bimodal peak becomes less pronounced, as the minimum duration of MLCs increases.

It can be argued that a close relationship between MLCs and snow cover extent is

expected because winter MLCs are likely to deposit snow. Generally, MLCs during the winter will deposit snow on their north side and produce non-frozen precipitation south of their center. This precipitation pattern would produce the relationship seen; the MLC center is just south of the snow cover extent. However, lagged analysis shows that it is pre-existing snow cover that is related to the MLC trajectories. The differences between snow cover and MLCs on the same day versus snow cover two days before the MLCs are small. This is highly suggestive that it is not snow being produced by the MLC itself. In addition, the relationship with the MLC leading the snow cover is consistent with the expectation of snow being produced to the north of the center and non-frozen precipitation to the south. With the MLCs leading the snow cover by two days there is a shift toward the left in the distributions, indicative of the center moving closer to the snow edge. This is likely snow deposited by the MLC itself.

It is difficult to determine the significance of the enhanced peaks near the snow extent because there is no a priori distribution that is expected. To attempt to prove the enhanced peaks near the snow extent are significant and not a random occurrence, we computed distributions of the distance between snow cover extent and MLCs using snow cover from all other years as a way to shuffle the datasets. Summing the distributions should result in any random noise canceling out. The most coherent structures in the differences occur in a region 50-350 km south of the snow extent. Outside of the region south of the boundary, the structures in the differences are not coherent and are of smaller magnitude. The structures suggest that MLCs in the region just south of the boundary are closely tied to the snow cover extent for the same year. Therefore, the relationship between MLC centers and the snow cover extent must have a physical link. A stronger relationship in the spring is also seen. The peaks observed in the distributions of distances are largest and the robustness analysis has the largest and most coherent structures during the spring. This may be attributed to increasing incident solar radiation

during the spring. The increase in solar radiation will in turn increase the temperature contrast between the snow-covered ground and the bare-ground. Segal et al. (1991b) found that the "snow breeze" was strongest during the spring for this very reason. A "snow breeze" type circulation and increasing solar radiation resulting in a temperature contrast are two physical processes that can link the snow cover extent to the MLCs. As additional evidence toward robustness of the result, the distance relationship is similar to the distributions seen using the Atlas of Extratopical Storm Tracks (Chandler and Jonas, 1999) instead of our NARR derived storm positions.

4.3 Physical Mechanism

The commonly postulated (e.g., Namias, 1962; Ross and Walsh, 1986) mechanism for the relationship between mid-latitude cyclone tracks and snow cover extent is one that is based on a region of enhanced low-level baroclinicity along the snow cover extent. The enhanced temperature and moisture gradient setup from the change in surface properties induces a temperature gradient between the snow covered and the ground without snow cover. The temperature gradient is a result of a large gradient in surface albedo that leads to a large difference in absorbed incident solar radiation. The increased temperature gradient across the snow extent line is then believed to lead to enhanced low-level baroclinicity. Regions of enhanced baroclinicity are more favorable for MLCs because the eddy growth rate is enhanced.

The results show that the largest mean baroclinicity values, relative to the snow extent, are in a region just south of the snow extent. The area of enhanced baroclinicity is much broader (from approximately the snow extent to 800 km south of the snow extent) than the peaks observed in MLC cycle frequency relative to the snow extent that tended to be very pronounced and limited to a few hundred kilometers. The region of largest baroclinicity just south of the snow extent provides support for the mechanism

proposed in Namias (1962) and Ross and Walsh (1986). The region immediately south of the snow extent will experience maximum eddy growth rates making it a region that is favorable for MLCs to develop and grow. The region of maximum growth rate is analogous to the region of maximum baroclinic instability. It is expected that MLCs will tend to follow regions of maximum baroclinic instability because it is the primary driving mechanism for them. The region of maximum eddy growth rates coupled with the same region experiencing maximum cyclone frequency signals that the two are related. It is not clear from our analysis how this low-level baroclinicity is realized at upper levels. We speculate that a pre-existing disturbance at upper-levels is need in order to realize the enhanced baroclinicity at low-levels. The low-level baroclinicity will modify the structure of the MLC resulting in trajectory changes. More work is needed to understand why the MLC centers are seen in a region 50-350 km south of the snow extent while the region of maximum baroclinic instability does not always peak in that region and has a much broader structure.

With ACC, snow cover extent is expected to decrease (Brown and Mote, 2009) due to rising global temperatures and there is an observed (IPCC, 2007; Sickmoller et al., 2000; Wang et al., 2006) and forecast (Bengtsson et al., 2006; Jiang and Perrie, 2007) northward shift in storm tracks (mainly over the North Atlantic and North Pacific). If the relationship between MLC centers and snow cover extent remains constant with ACC, then a northward shift of MLCs over continents would be expected given a shift northward in snow cover extent. The shift northward of snow cover over continents may also play a role in the northward shift seen in the ocean basins east of continents. Hoskins and Valdes (1990) demonstrated that increased baroclinicity generated off the east coast of continents was important to the start of storm tracks in those regions. Ross and Walsh (1986) found that enhanced baroclinicity near coastal boundaries due to increased snow cover is important to MLC trajectories. Therefore, as snow cover

extent moves northward over continents we speculate that this will move the region of enhanced baroclinicity at the coast northward too. With this northward shift and that the North Atlantic and North Pacific storm tracks are sensitive to the region of enhanced baroclinicity we postulate that snow cover retreat over continents may play a role in the northward shift seen in ocean basins.

5 Conclusion

A MLC identification and tracking method was developed using high temporal and spatial resolution NARR output. A simple algorithm for determining the southern extent of snow cover in North America was created so the MLC centers could be compared to it. Investigation of the role snow cover extent has on MLC trajectories showed that there is an enhanced region of MLC frequency 50-350 km south of the snow cover extent. The relationship appears to be driven by low-level baroclinicity that is at its maximum in this region. Increased low-level baroclinicity is believed to be driven by the increased temperature gradient across the boundary due to differences in absorbed solar radiation. The relationship between MLC centers and snow cover extent is shown to be robust by shuffling years of snow cover and showing that the largest and most coherent changes occur in the region of enhanced MLC frequency. In addition, the relationship is insensitive to the MLC database used. The close relationship between MLC centers and snow cover extent may play a role in the northward shift of storm tracks seen with ACC. Snow cover is found to lead the MLC centers, and thus with a northward retreat of snow cover extent due to ACC we expect a similar northward shift in MLC tracks over the North American continent.

5.1 Future Work

Now that a statistical relationship has been shown, it will be useful to further investigate the relationship using a numerical model. A numerical model will reduce a lot of the uncertainty of the statistical analysis because a better cause and effect relationship can be established. In addition, it will allow us to explain why the MLC center is where it is given the location of the enhanced low-level baroclinicity. There are two setups we feel will be useful in studying the relationship further. The first is to use an idealized MLC with no topography. This type of experiment will allow varying distances of snow

cover extent from the mid-latitude cyclone center. The MLCs can be tracked, using a similar algorithm presented in this paper or a more sophisticated one because it will be less computationally intensive, and compared for varying degrees of snow cover extent. Comparing the snow covered runs to a bare-ground control run will allow one to see how the trajectory is modified due to the snow cover feedbacks. The second is to do reanalysis of real MLCs with varying degrees of snow cover. This is very similar to the work of Elguindi et al. (2005), but with the important difference that it is small variations of snow cover extent. This type of experiment will allow topography and other feedbacks not in the idealized case to have an impact. We hypothesize that in the real world case there will be less of a change in MLC trajectory than in the idealized case because of the increased complexity of the system. It has also been suggested that some of the analysis we have performed be segregated beyond just months to see if the relationship is stronger or weaker in certain situations than others. For example, one can separate the results by ENSO phases to see if ENSO plays a significant role in the relationship. Also, looking at the relationship segregated by mean latitude of the snow extent line may provide some interesting results related to any climatological factors driving the relationship or if our relationship is only from storms like the ones discussed in Namias (1962) (when the snow cover extent it near coastal boundaries). A better understanding of the physical processes involved will allow for a better assessment of what changes to MLC trajectories can be expected with ACC.

References

Alexander, P. and G. Gong, 2011: Modeled surface air temperature response to snow depth variability. *Journal of Geophysical Research*, **116 (D14)**, 1–14, doi:10.1029/2010JD014908.

Allen, R. J. and C. S. Zender, 2011a: Forcing of the Arctic Oscillation by Eurasian Snow Cover. *Journal of Climate*, **24 (24)**, 6528–6539, doi:10.1175/2011JCLI4157.1.

Allen, R. J. and C. S. Zender, 2011b: The role of eastern Siberian snow and soil moisture anomalies in quasi-biennial persistence of the Arctic and North Atlantic Oscillations. *Journal of Geophysical Research*, **116 (D16)**, 1–12, doi:10.1029/2010JD015311.

Alpert, P., B. U. Neeman, and Y. Shay-El, 1990: Climatological analysis of Mediterranean cyclones using ECMWF data. *Tellus A*, **42 (1)**, 65–77, doi:10.1034/j.1600-0870.1990.00007.x.

Baker, D. G., D. L. Ruschy, R. H. Skaggs, and D. B. Wall, 1992: Air Temperature and Radiation Depressions Associated with a Snow Cover. *Journal of Applied Meteorology*, **31 (3)**, 247–254, doi:10.1175/1520-0450(1992)031⟨0247:ATARDA⟩2.0.CO;2.

Barrett, A., 2003: National Operational Hydrologic Remote Sensing Center Snow Data Assimilation System (SNODAS) Products at NSIDC. SIDC Special Report 11. Tech. rep., National Snow and Ice Data Center, 19 pp., Boulder, CO.

Bauer, K. G. and J. a. Dutton, 1962: Albedo Variations Measured from an Airplane over Several Types of Surface. *Journal of Geophysical Research*, **67 (6)**, 2367–2376, doi:10.1029/JZ067i006p02367.

Bauer, M. and A. D. Del Genio, 2006: Composite Analysis of Winter Cyclones in a GCM: Influence on Climatological Humidity. *Journal of Climate*, **19 (9)**, 1652–1672, doi:10.1175/JCLI3690.1.

BENESTAD, R. E. and D. CHEN, 2006: The use of a calculus-based cyclone identification method for generating storm statistics. *Tellus A*, **58 (4)**, 473–486, doi:10.1111/j.1600-0870.2006.00191.x.

Bengtsson, L., K. I. Hodges, and E. Roeckner, 2006: Storm Tracks and Climate Change. *Journal of Climate*, **19 (15)**, 3518–3543, doi:10.1175/JCLI3815.1.

Blackmon, M. L., 1976: A Climatological Spectral Study of the 500 mb Geopotential Height of the Northern Hemisphere. *Journal of the Atmospheric Sciences*, **33 (8)**, 1607–1623, doi:10.1175/1520-0469(1976)033⟨1607:ACSSOT⟩2.0.CO;2.

Blender, R., K. Fraedrich, and F. Lunkeit, 1997: Identification of cyclone-track regimes in the North Atlantic. *Quarterly Journal of the Royal Meteorological Society*, **123 (539)**, 727–741, doi:10.1002/qj.49712353910.

Blender, R. and M. Schubert, 2000: Cyclone Tracking in Different Spatial and Temporal Resolutions. *Monthly Weather Review*, **128 (2)**, 377, doi:10.1175/1520-0493(2000)128⟨0377:CTIDSA⟩2.0.CO;2.

Brown, R. D., 2000: Northern Hemisphere Snow Cover Variability and Change, 191597. *Journal of Climate*, **13 (13)**, 2339–2355, doi:10.1175/1520-0442(2000)013⟨2339:NHSCVA⟩2.0.CO;2.

Brown, R. D. and R. L. Armstrong, 2008: Snow-cover data: measurment, products, and sources. *Snow and Climate: Physical Processes, Surface Energy Exchange and Modeling*, R. Armstrong and E. Brun, Eds., Cambridge University Press, New York, NY, chap. 5, 181–216.

Brown, R. D. and P. W. Mote, 2009: The Response of Northern Hemisphere Snow Cover to a Changing Climate*. *Journal of Climate*, **22 (8)**, 2124–2145, doi:10.1175/2008JCLI2665.1.

Cannon, A. J., 2012: Regression-Guided Clustering: A Semisupervised Method for Circulation-to-Environment Synoptic Classification. *Journal of Applied Meteorology and Climatology*, **51 (2)**, 185–190, doi:10.1175/JAMC-D-11-0155.1.

Chandler, M. and J. Jonas, 1999: Atlas of extratropical storm tracks (1961-1998). Tech. rep. URL `http://www.giss.nasa.gov/data/stormtracks`.

Chang, A. T. C., J. Foster, and D. K. Hall, 1987: Nimbus-7 SMMR derived global snow cover parameters. *Annals of Glaciology*, **9**, 39–44.

Chang, E. K. M., S. Lee, and K. L. Swanson, 2002: Storm Track Dynamics. *Journal of Climate*, **15 (16)**, 2163–2183, doi:10.1175/1520-0442(2002)015⟨02163:STD⟩2.0.CO;2.

Cohen, J. and D. Entekhabi, 2001: The influence of snow cover on northern hemisphere climate variability. *Atmosphere-Ocean*, **39 (1)**, 35–53, doi:10.1080/07055900.2001.9649665.

Cohen, J. and D. Rind, 1991: The Effect of Snow Cover on the Climate. *Journal of Climate*, **4 (7)**, 689–706, doi:10.1175/1520-0442(1991)004⟨0689:TEOSCO⟩2.0.CO;2.

Déry, S. J. and R. D. Brown, 2007: Recent Northern Hemisphere snow cover extent trends and implications for the snow-albedo feedback. *Geophysical Research Letters*, **34 (22)**, 2–7, doi:10.1029/2007GL031474.

Dewey, K. F., 1977: Daily Maximum and Minimum Temperature Forecasts and the Influence of Snow Cover. *Monthly Weather Review*, **105 (12)**, 1594–1597, doi:10.1175/1520-0493(1977)105⟨1594:DMAMTF⟩2.0.CO;2.

Dutra, E., C. Schär, P. Viterbo, and P. M. a. Miranda, 2011: Land-atmosphere coupling associated with snow cover. *Geophysical Research Letters*, **38 (15)**, 1–5, doi:10.1029/2011GL048435.

Elguindi, N., B. Hanson, and D. Leathers, 2005: The Effects of Snow Cover on Midlatitude Cyclones in the Great Plains. *Journal of Hydrometeorology*, **6 (3)**, 263–279, doi:10.1175/JHM415.1.

Ellis, A. W. and D. J. Leathers, 1998: The effects of a discontinuous snow cover on lower atmospheric temperature and energy flux patterns. *Geophysical Research Letters*, **25 (12)**, 2161, doi:10.1029/98GL01582.

Ellis, A. W. and D. J. Leathers, 1999: Analysis of Cold Airmass Temperature Modification across the U.S. Great Plains as a Consequence of Snow Depth and Albedo. *Journal of Applied Meteorology*, **38 (6)**, 696–711, doi:10.1175/1520-0450(1999)038⟨0696:AOCATM⟩2.0.CO;2.

Finnis, J., M. M. Holland, M. C. Serreze, and J. J. Cassano, 2007: Response of Northern Hemisphere extratropical cyclone activity and associated precipitation to climate change, as represented by the Community Climate System Model. *Journal of Geophysical Research*, **112 (G4)**, 1–14, doi:10.1029/2006JG000286.

Fletcher, C. G., S. C. Hardiman, P. J. Kushner, and J. Cohen, 2009: The Dynamical Response to Snow Cover Perturbations in a Large Ensemble of Atmospheric GCM Integrations. *Journal of Climate*, **22 (5)**, 1208–1222, doi:10.1175/2008JCLI2505.1.

Frei, A., D. a. Robinson, and M. G. Hughes, 1999: North American snow extent: 19001994. *International Journal of Climatology*, **19 (14)**, 1517–1534, doi:10.1002/(SICI)1097-0088(19991130)19:14⟨1517::AID-JOC437⟩3.3.CO;2-9.

Geng, Q. and M. Sugi, 2001: Variability of the North Atlantic Cyclone Activity in Winter Analyzed from NCEPNCAR Reanalysis Data. *Journal of Climate*, **14 (18)**, 3863–3873, doi:10.1175/1520-0442(2001)014⟨3863:VOTNAC⟩2.0.CO;2.

Grigoriev, S., S. Gulev, and O. Zolina, 2000: Innovative software facilitates cyclone tracking and analysis. *Eos, Transactions American Geophysical Union*, **81 (16)**, 170–170, doi:10.1029/00EO00117.

Grody, N. and A. Basist, 1996: Global identification of snowcover using SSM/I measurements. *IEEE Transactions on Geoscience and Remote Sensing*, **34 (1)**, 237–249, doi:10.1109/36.481908.

Gulev, S. K., O. Zolina, and S. Grigoriev, 2001: Extratropical cyclone variability in the Northern Hemisphere winter from the NCEP/NCAR reanalysis data. *Climate Dynamics*, **17 (10)**, 795–809, doi:10.1007/s003820000145.

Haak, U. and U. Ulbrich, 1996: Verification of an objective cyclone climatology for the North Atlantic. *Meteorologische Zeitschrift*, **5**, 24–30.

Hall, D. K., G. A. Riggs, and V. V. Salomonson, 1995: Development of methods for mapping global snow cover using moderate resolution imaging spectroradiometer data. *Remote Sensing of Environment*, **54 (2)**, 127–140, doi:10.1016/0034-4257(95)00137-P.

Hewson, T. D. and H. a. Titley, 2010: Objective identification, typing and tracking of the complete life-cycles of cyclonic features at high spatial resolution. *Meteorological Applications*, **17 (3)**, 355–381, doi:10.1002/met.204.

Hodges, K. I., 1994: A General Method for Tracking Analysis and Its Application to Meteorological Data. *Monthly Weather Review*, **122 (11)**, 2573–2586, doi:10.1175/1520-0493(1994)122⟨2573:AGMFTA⟩2.0.CO;2.

Hodges, K. I., B. J. Hoskins, J. Boyle, and C. Thorncroft, 2003: A Comparison of Recent Reanalysis Datasets Using Objective Feature Tracking: Storm Tracks and Tropical Easterly Waves. *Monthly Weather Review*, **131 (9)**, 2012–2037, doi:10.1175/1520-0493(2003)131⟨2012:ACORRD⟩2.0.CO;2.

Hoskins, B. J. and K. I. Hodges, 2002: New Perspectives on the Northern Hemisphere Winter Storm Tracks. *Journal of the Atmospheric Sciences*, **59 (6)**, 1041–1061, doi:10.1175/1520-0469(2002)059⟨1041:NPOTNH⟩2.0.CO;2.

Hoskins, B. J. and P. J. Valdes, 1990: On the Existence of Storm-Tracks. *Journal of the Atmospheric Sciences*, **47 (15)**, 1854–1864, doi:10.1175/1520-0469(1990)047⟨1854:OTEOST⟩2.0.CO;2.

Inatsu, M., 2009: The neighbor enclosed area tracking algorithm for extratropical wintertime cyclones. *Atmospheric Science Letters*, **272 (October)**, n/a–n/a, doi:10.1002/asl.238.

IPCC, 2007: *Climate Change 2007: The Physical Science Basis. Contribution of Working Group I to the Fourth Assessment Report of the Intergovernmental Panel on Cliamte Change*. Cambridge University Press, New York, NY, 996 pp.

Jiang, J. and W. Perrie, 2007: The Impacts of Climate Change on Autumn North Atlantic Midlatitude Cyclones. *Journal of Climate*, **20 (7)**, 1174–1187, doi:10.1175/JCLI4058.1.

Johnson, R. H., G. S. Young, J. J. Toth, and R. M. Zehr, 1984: Mesoscale Weather Effects of Variable Snow Cover over Northeast Colorado. *Monthly Weather Review*, **112 (6)**, 1141–1152, doi:10.1175/1520-0493(1984)112⟨1141:MWEOVS⟩2.0.CO;2.

Kaspi, Y. and T. Schneider, 2011: Downstream Self-Destruction of Storm Tracks. *Journal of the Atmospheric Sciences*, **68 (10)**, 2459–2464, doi:10.1175/JAS-D-10-05002.1.

Klein, W., 1957: *Principal Tracks and Mean Frequencies of Cyclones and Anticyclones in the Northern Hemisphere, Research Paper No. 40*. U.S. Weather Bureau, Washington, DC.

Klingaman, N. P., B. Hanson, and D. J. Leathers, 2008: A Teleconnection between Forced Great Plains Snow Cover and European Winter Climate. *Journal of Climate*, **21 (11)**, 2466–2483, doi:10.1175/2007JCLI1672.1.

König, W., R. Sausen, and F. Sielmann, 1993: Objective Identification of Cyclones in GCM Simulations. *Journal of Climate*, **6 (12)**, 2217–2231, doi:10.1175/1520-0442(1993)006⟨2217:OIOCIG⟩2.0.CO;2.

Kopp, T. J. and R. B. Kiess, 1996: The Air Force Global Weather Central Snow analysis Model. *15th Conf. on Weather Analysis and Forecasting*, Amer. Meteor. Soc., Norfolk, VA, 220–222.

Kunkel, K. E., M. a. Palecki, K. G. Hubbard, D. a. Robinson, K. T. Redmond, and D. R. Easterling, 2007: Trend Identification in Twentieth-Century U.S. Snowfall: The Challenges. *Journal of Atmospheric and Oceanic Technology*, **24 (1)**, 64–73, doi:10.1175/JTECH2017.1.

Lambert, S. J., 1988: A Cyclone Climatology of the Canadian Climate Centre General Circulation Model. *Journal of Climate*, **1 (1)**, 109–115, doi:10.1175/1520-0442(1988)001⟨0109:ACCOTC⟩2.0.CO;2.

Leathers, D. J., T. L. Mote, A. J. Grundstein, D. a. Robinson, K. Felter, K. Conrad, and L. Sedywitz, 2002: Associations between continental-scale snow cover anomalies and air mass frequencies across eastern North America. *International Journal of Climatology*, **22 (12)**, 1473–1494, doi:10.1002/joc.807.

Lindzen, R. S. and B. Farrell, 1980: A Simple Approximate Result for the Maximum Growth Rate of Baroclinic Instabilities. *Journal of the Atmospheric Sciences*, **37 (7)**, 1648–1654, doi:10.1175/1520-0469(1980)037⟨1648:ASARFT⟩2.0.CO;2.

Lionello, P., F. Dalan, and E. Elvini, 2002: Cyclones in the Mediterranean region: the present and the doubled CO2 climate scenarios. *Climate Research*, **22**, 147–159, doi:10.3354/cr022147.

Long, Z., W. Perrie, J. Gyakum, R. Laprise, and D. Caya, 2009: Scenario changes in the climatology of winter midlatitude cyclone activity over eastern North America and the Northwest Atlantic. *Journal of Geophysical Research*, **114 (D12)**, 1–13, doi:10.1029/2008JD010869.

Matson, M. and D. R. Wiesnet, 1981: New data base for climate studies. *Nature*, **289 (5797)**, 451–456, doi:10.1038/289451a0.

Matsumura, S. and K. Yamazaki, 2012: Eurasian Subarctic Summer Climate in Response to Anomalous Snow Cover. *Journal of Climate*, **25 (4)**, 1305–1317, doi:10.1175/2011JCLI4116.1.

Matsumura, S., K. Yamazaki, and T. Tokioka, 2010: Summertime land-atmosphere interactions in response to anomalous springtime snow cover in northern Eurasia. *Journal of Geophysical Research*, **115 (D20)**, 1–13, doi:10.1029/2009JD012342.

Mesinger, F., et al., 2006: North American Regional Reanalysis. *Bulletin of the American Meteorological Society*, **87 (3)**, 343–360, doi:10.1175/BAMS-87-3-343.

Mote, T. L., 2008: On the Role of Snow Cover in Depressing Air Temperature. *Journal of Applied Meteorology and Climatology*, **47 (7)**, 2008–2022, doi:10.1175/2007JAMC1823.1.

Murray, R. and I. Simmonds, 1991: A numerical scheme for tracking cyclone centres from digital data. Part I: Development and operation of the scheme. *Australian Meteorological Magazine*, **39 (3)**, 155–166.

Namias, J., 1962: Influences of abnormal heat sources and sinks on atmospheric behavior. *Int. Symp. on Numerical Weather Prediction*, Meteorological Society of Japan, Tokyo, Japan, 615–627.

Namias, J., 1978: Multiple Causes of the North American Abnormal Winter 197677. *Monthly Weather Review*, **106 (3)**, 279–295, doi:10.1175/1520-0493(1978)106⟨0279:MCOTNA⟩2.0.CO;2.

Namias, J., 1985: Some Empirical Evidence for the Influence of Snow Cover on Temperature and Precipitation. *Monthly Weather Review*, **113 (9)**, 1542–1553, doi:10.1175/1520-0493(1985)113⟨1542:SEEFTI⟩2.0.CO;2.

National Centers for Environmental Prediction, 2007: Regional Reanalysis Questions and Answers. URL `http://www.emc.ncep.noaa.gov/mmb/rreanl/faq.html`, URL `http://www.emc.ncep.noaa.gov/mmb/rreanl/faq.html`.

Nghiem, S., 2001: Global snow cover monitoring with spaceborne K/sub u/-band scatterometer. *IEEE Transactions on Geoscience and Remote Sensing*, **39 (10)**, 2118–2134, doi:10.1109/36.957275.

Ross, B. and J. E. Walsh, 1986: Synoptic-Scale Influences of Snow Cover and Sea Ice. *Monthly Weather Review*, **114 (10)**, 1795–1810, doi:10.1175/1520-0493(1986)114⟨1795:SSIOSC⟩2.0.CO;2.

Segal, M., J. H. Cramer, R. A. Pielke, J. R. Garratt, and P. Hildebrand, 1991a: Observational Evaluation of the Snow Breeze. *Monthly Weather Review*, **119 (2)**, 412–424, doi:10.1175/1520-0493(1991)119⟨0412:OEOTSB⟩2.0.CO;2.

Segal, M., J. R. Garratt, R. A. Pielke, and Z. Ye, 1991b: Scaling and Numerical Model Evaluation of Snow-Cover Effects on the Generation and Modification of Daytime Mesoscale Circulations. *Journal of the Atmospheric Sciences*, **48 (8)**, 1024–1042, doi:10.1175/1520-0469(1991)048⟨1024:SANMEO⟩2.0.CO;2.

Sickmoller, M., R. Blender, and K. Fraedrich, 2000: Observed winter cyclone tracks in the northern hemisphere in re-analysed ECMWF data. *Quarterly Journal of the Royal Meteorological Society*, **126 (563)**, 591–620, doi:10.1256/smsqj.56310.

Sinclair, M. R., 1997: Objective Identification of Cyclones and Their Circulation Intensity, and Climatology. *Weather and Forecasting*, **12 (3)**, 595–612, doi:10.1175/1520-0434(1997)012⟨0595:OIOCAT⟩2.0.CO;2.

Sobolowski, S., G. Gong, and M. Ting, 2007: Northern Hemisphere winter climate variability: Response to North American snow cover anomalies and orography. *Geophysical Research Letters*, **34 (16)**, 2–6, doi:10.1029/2007GL030573.

Sobolowski, S., G. Gong, and M. Ting, 2010: Modeled Climate State and Dynamic Responses to Anomalous North American Snow Cover. *Journal of Climate*, **23 (3)**, 785–799, doi:10.1175/2009JCLI3219.1.

Sobolowski, S., G. Gong, and M. Ting, 2011: Investigating the Linear and Nonlinear Stationary Wave Response to Anomalous North American Snow Cover. *Journal of the Atmospheric Sciences*, **68 (4)**, 904–917, doi:10.1175/2010JAS3581.1.

Taylor, C. M., R. J. Harding, R. A. Pielke, P. L. Vidale, R. L. Walko, and J. W. Pomeroy, 1998: Snow breezes in the boreal forest. *Journal of Geophysical Research*, **103 (D18)**, 23 087–23 101, doi:10.1029/98JD02004.

Thomas, B. C. and J. E. Martin, 2007: A Synoptic Climatology and Composite Analysis of the Alberta Clipper. *Weather and Forecasting*, **22 (2)**, 315–333, doi:10.1175/WAF982.1.

Ulbrich, U., G. C. Leckebusch, and J. G. Pinto, 2009: Extra-tropical cyclones in the present and future climate: a review. *Theoretical and Applied Climatology*, **96 (1-2)**, 117–131, doi:10.1007/s00704-008-0083-8.

Vavrus, S., 2007: The role of terrestrial snow cover in the climate system. *Climate Dynamics*, **29 (1)**, 73–88, doi:10.1007/s00382-007-0226-0.

Wallace, J. M. and P. V. Hobbs, 2006: *Atmospheric science: an introductory survey*. 2d ed., International Geophysics Series 92, Academic press, 484 pp.

Walland, D. J. and I. Simmonds, 1996: Modelled atmospheric response to changes in Northern Hemisphere snow cover. *Climate Dynamics*, **13 (1)**, 25–34, doi:10.1007/s003820050150.

Walland, D. J. and I. Simmonds, 1997: North American and Eurasian snow cover covariability. *Tellus A*, **49 (4)**, 503–512, doi:10.1034/j.1600-0870.1997.t01-3-00007.x.

Walsh, J. E., 1984: Snow Cover and Atmospheric Variability: Changes in the snow covering the earth's surface affect both daily weather and long-term climate. *American Scientist*, **72 (1)**, 50–57.

Walsh, J. E., D. R. Tucek, and M. R. Peterson, 1982: Seasonal Snow Cover and Short-Term Climatic Fluctuations over the United States. *Monthly Weather Review*, **110 (10)**, 1474–1486, doi:10.1175/1520-0493(1982)110⟨1474:SSCAST⟩2.0.CO;2.

Wang, X. L., V. R. Swail, and F. W. Zwiers, 2006: Climatology and Changes of Extratropical Cyclone Activity: Comparison of ERA-40 with NCEPNCAR Reanalysis for 19582001. *Journal of Climate*, **19 (13)**, 3145–3166, doi:10.1175/JCLI3781.1.

Wojcik, G. S. and D. S. Wilks, 1992: Temperature Forecast Biases Associated with Snow Cover in the Northeast. *Weather and Forecasting*, **7 (3)**, 501–506, doi:10.1175/1520-0434(1992)007⟨0501:TFBAWS⟩2.0.CO;2.

Zhang, Y., T. Li, and B. Wang, 2004: Decadal Change of the Spring Snow Depth over the Tibetan Plateau: The Associated Circulation and Influence on the East Asian Summer Monsoon*. *Journal of Climate*, **17 (14)**, 2780–2793, doi:10.1175/1520-0442(2004)017⟨2780:DCOTSS⟩2.0.CO;2.

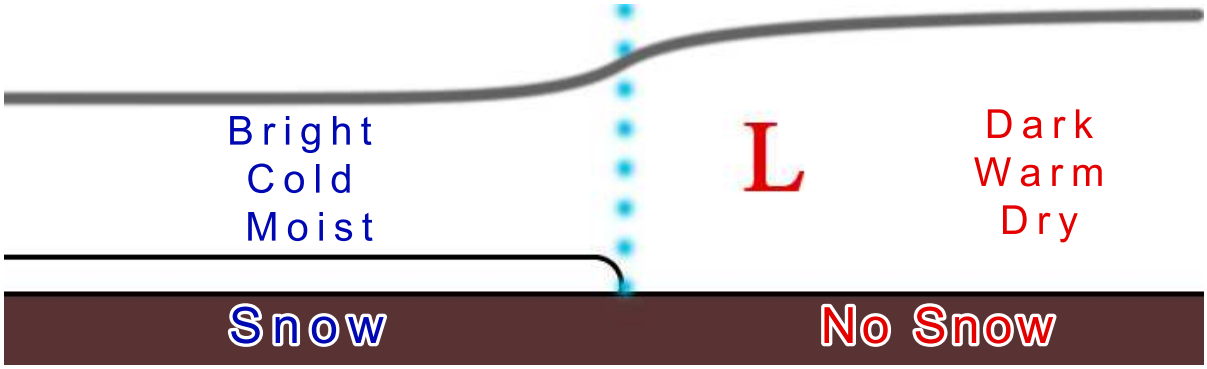

Figure 1: A simple schematic showing the properties induced by snow-covered ground and ground without snow-cover. The gray line is the estimated boundary layer height and the vertical dotted blue line is the snow cover extent boundary. The letter "L" is positioned in the region hypothesized for MLC centers to track based on enhanced baroclinicity near the snow extent.

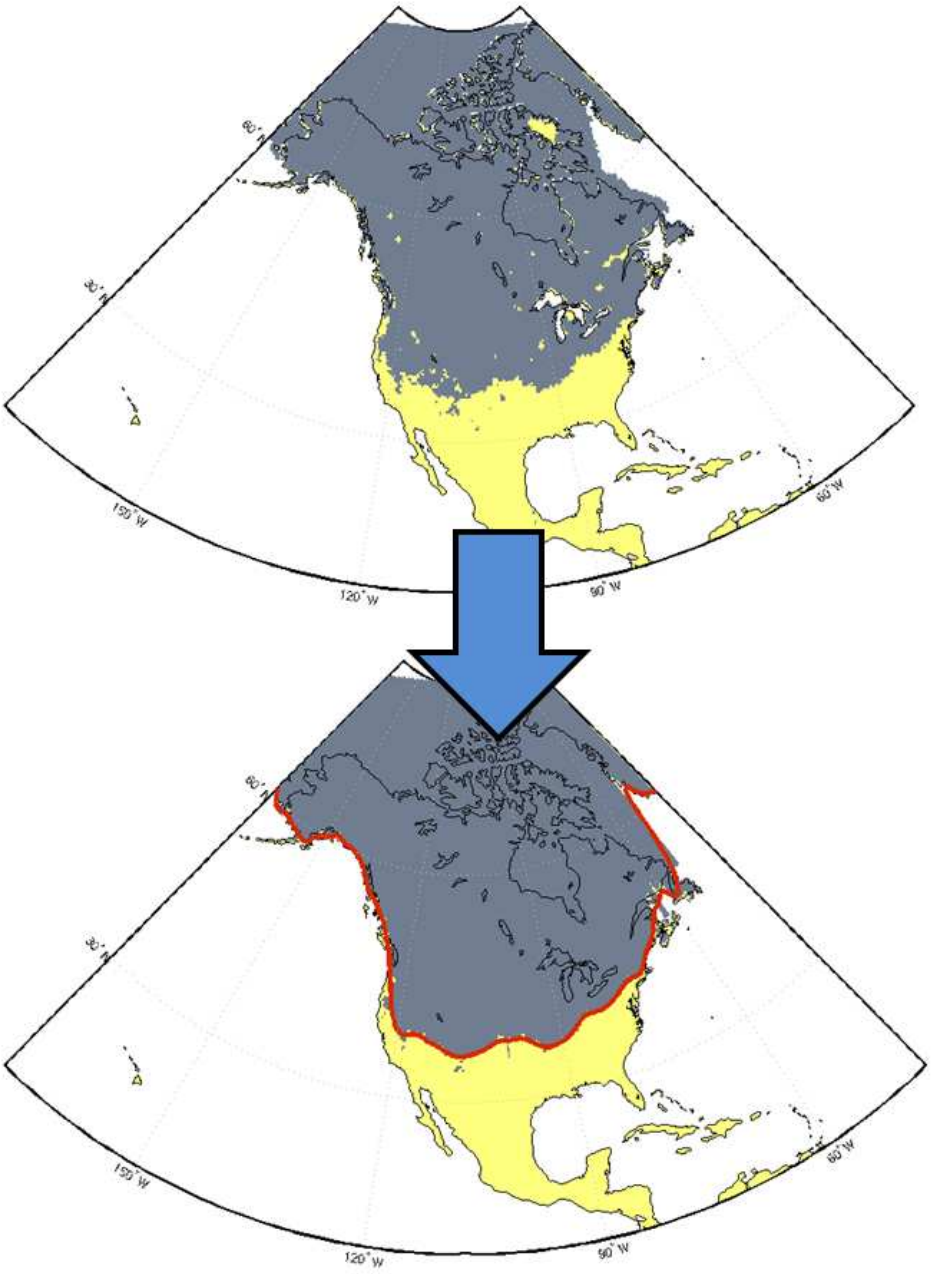

Figure 2: A sample day showing the raw snow cover extent (top) and the processed snow cover extent with the southern edge of the snow extent identified by our algorithm shown in red (bottom).

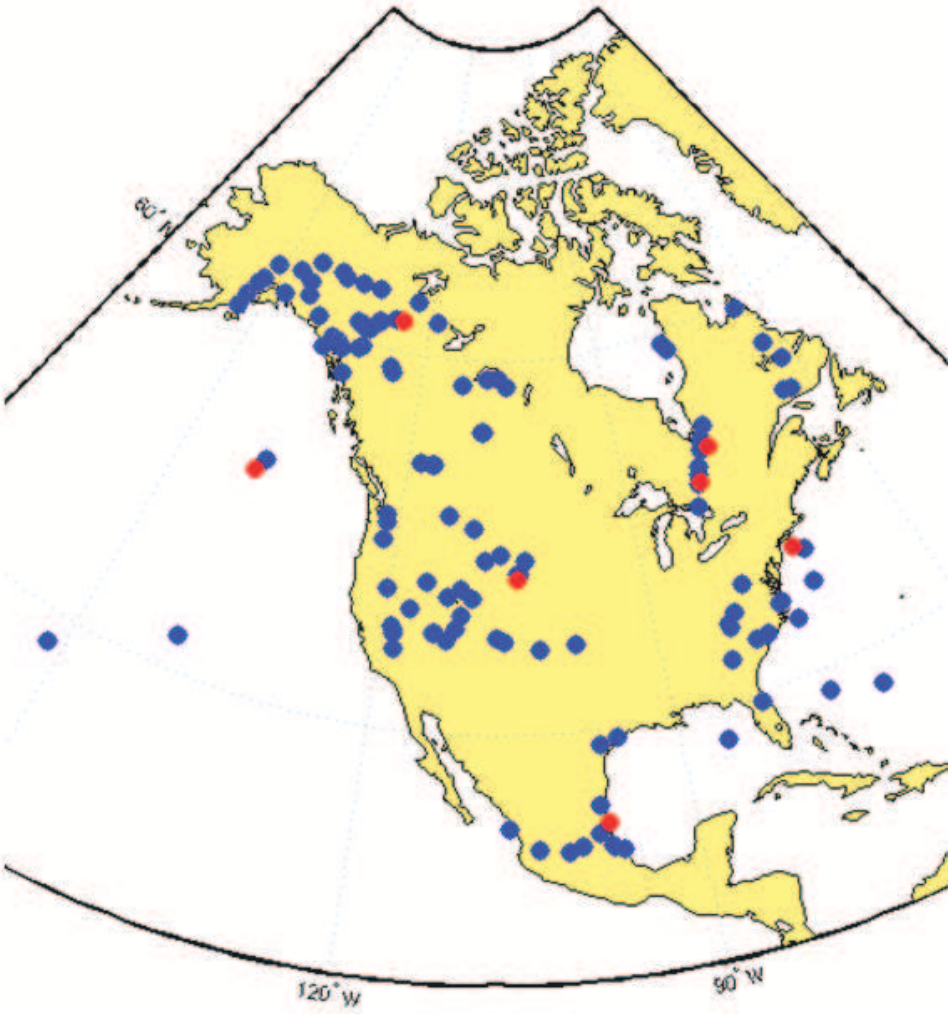

Figure 3: A sample identification of MLCs for a single day. The blue dots are pressure minima identified at a fine spatial resolution and the red dots are pressure minima identified at the coarse spatial resolution. The red dots are moved to the closest blue dot to determine the best estimate of the MLC center.

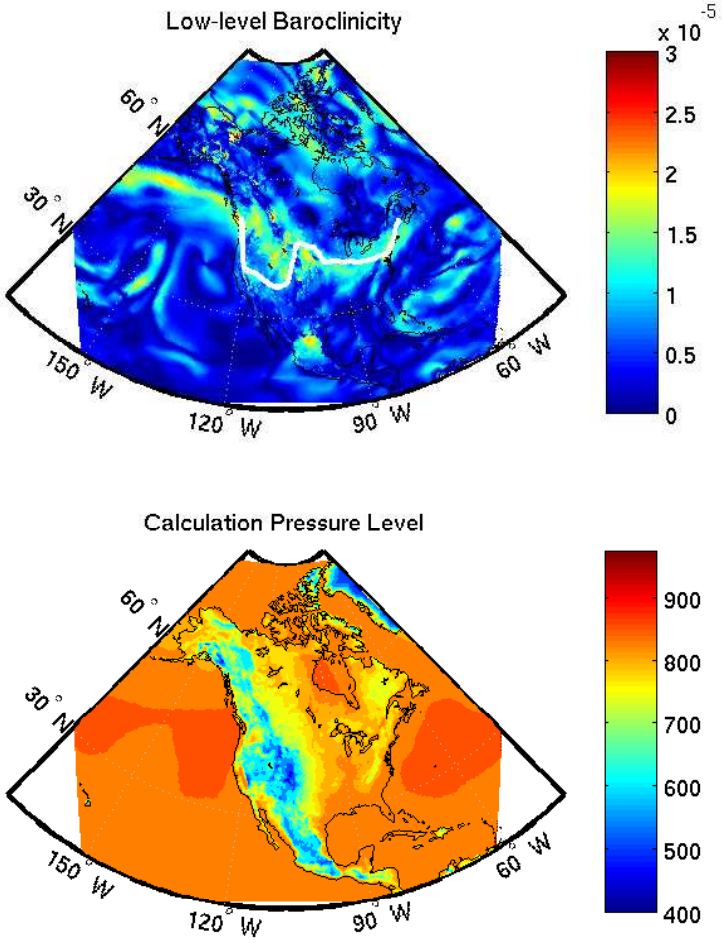

Figure 4: A sample low-level baroclinicity map for a single day. The top panel is the calculated low-level baroclinicity and the snow cover extent line is shown in white. The bottom panel is the pressure level at which the low-level baroclinicity was calculated at.

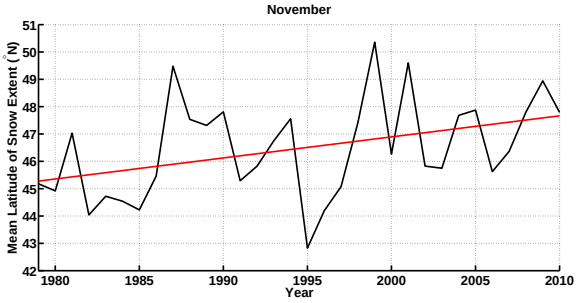

(a) November

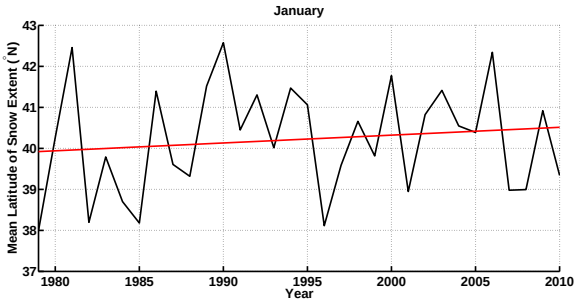

(b) January

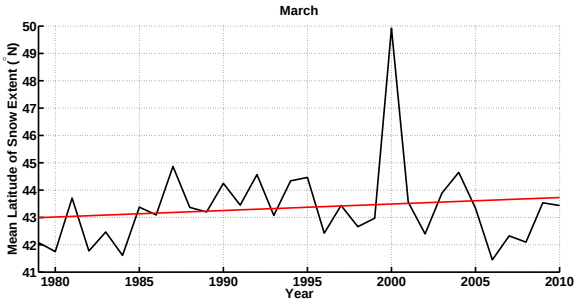

(c) March

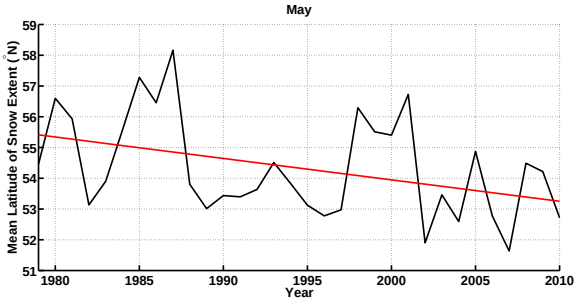

(d) May

Figure 5: Trends in mean latitude of snow cover extent in (a) November, (b) January,(c) March, and (d) May for 1979 to 2010. May and November are statistically significant at the 95% confidence level ($p = 0.02$ for both).

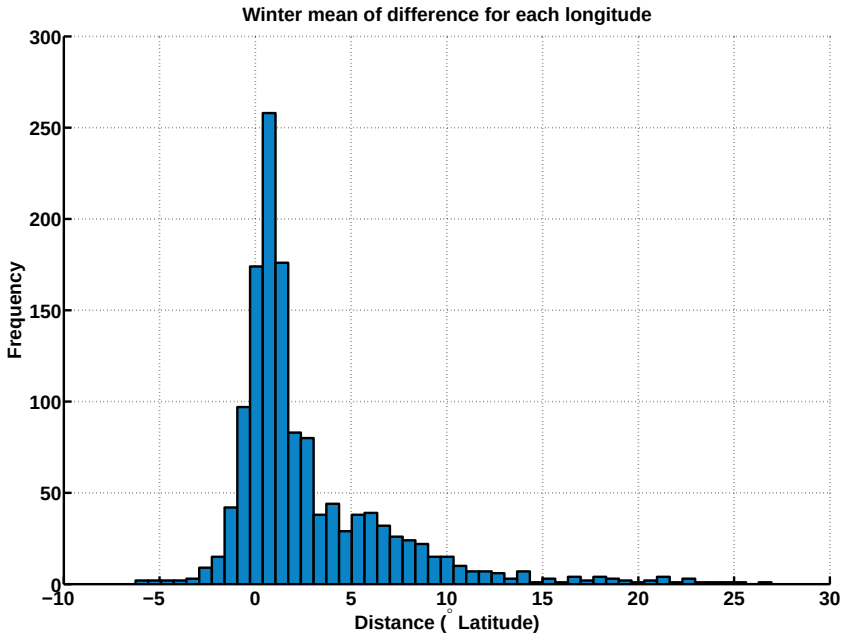

(a) October to May Mean of Difference

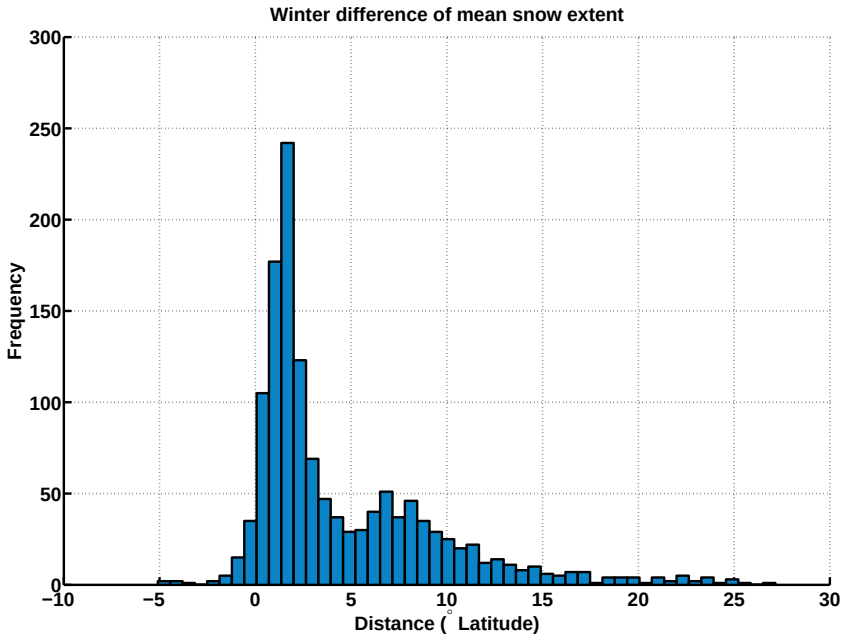

(b) October to May Difference of Mean

Figure 6: Comparison of our snow extent algorithm applied to NARR and SNODAS for 2004 to 2009. All differences are NARR snow extent minus SNODAS snow extent. (a) is the mean of the difference for each degree longitude and (b) is the difference of the mean latitudinal extent across all longitudes for October to May.

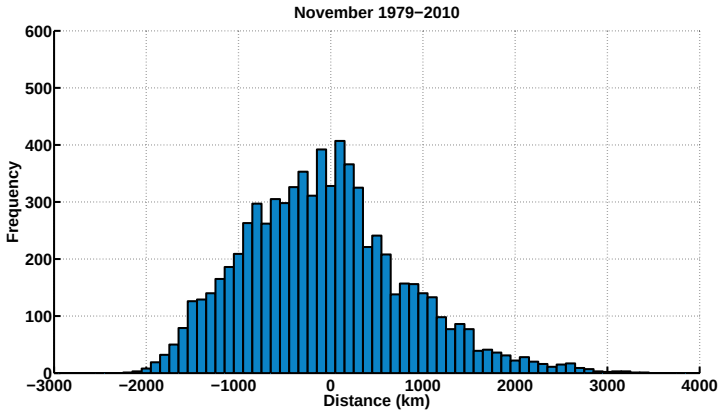

(a) November

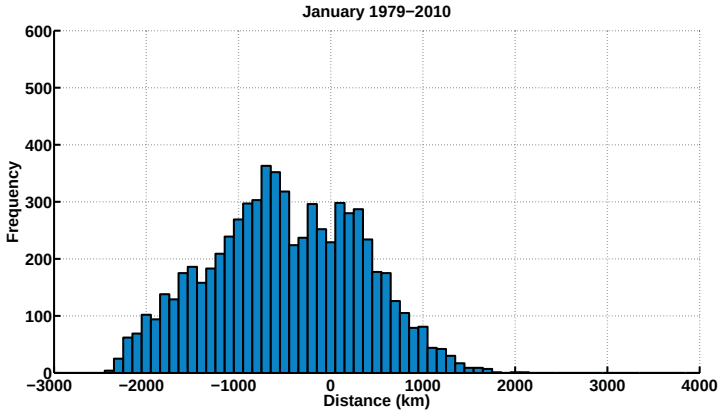

(b) January

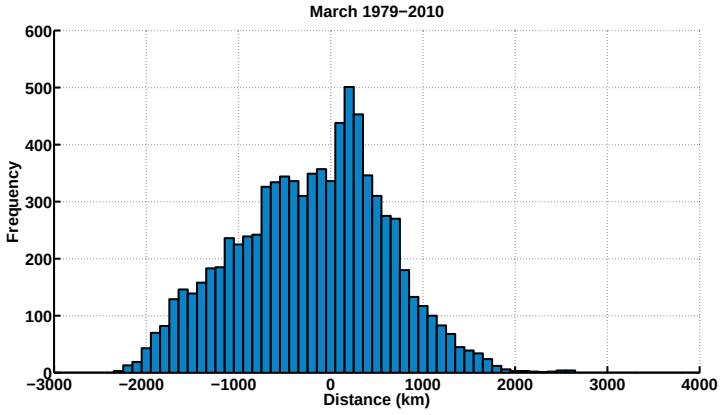

(c) March

Figure 7: MLC center distances from snow extent for storms lasting longer than 24 hrs in (a) November, (b) March, and (c) March for 1979 to 2010. Negative distances are MLC centers that are over snow and positive distances are MLC centers that are over ground without snow.

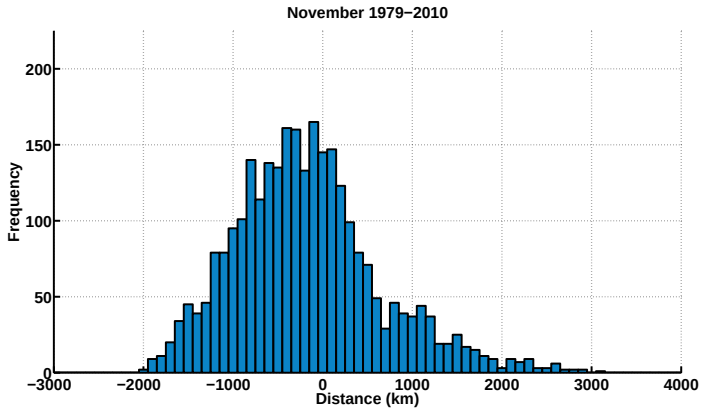

(a) November

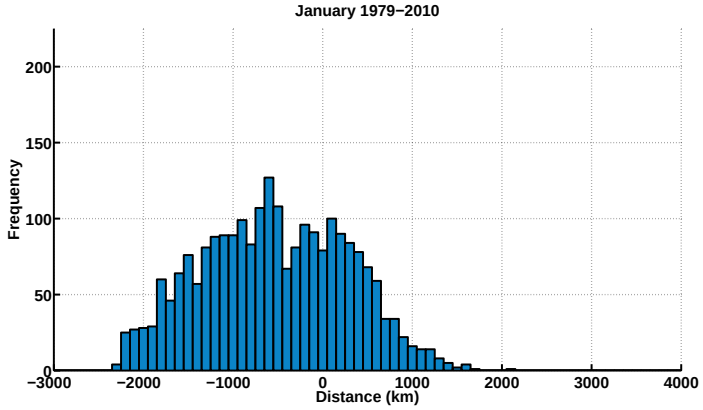

(b) January

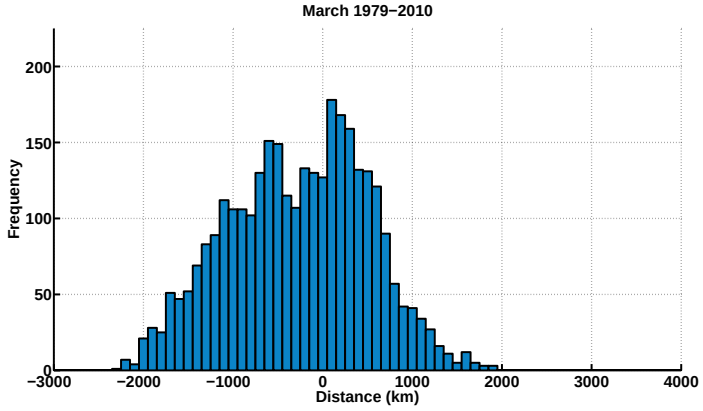

(c) March

Figure 8: MLC center distance from snow extent for storms lasting longer than 48 hrs in (a) November, (b) March, and (c) March for 1979 to 2010. Negative distances are MLC centers that are over snow and positive distances are MLC centers that are over ground without snow.

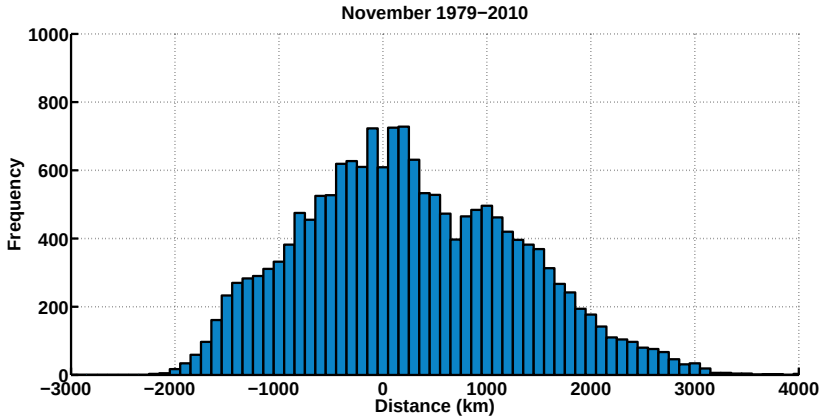

(a) November

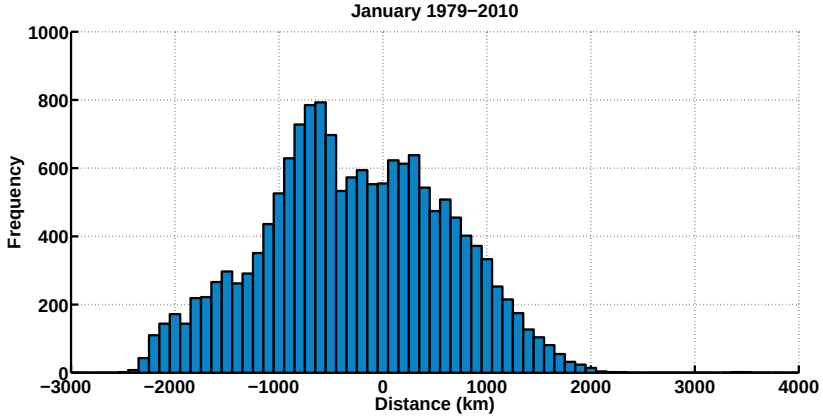

(b) January

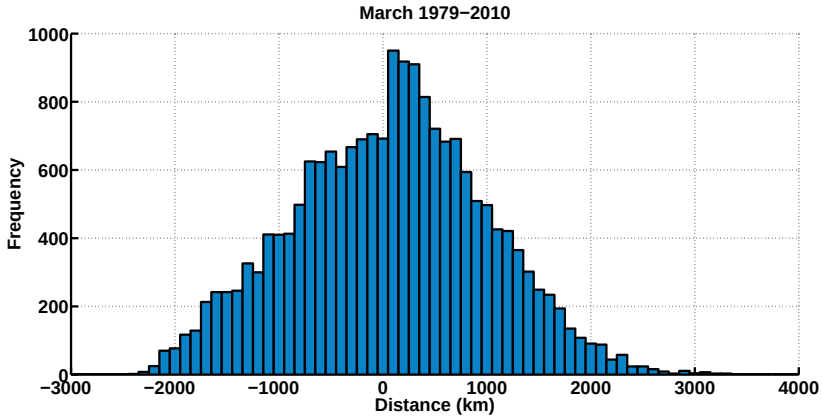

(c) March

Figure 9: MLC center distance from snow extent for storms lasting longer than 9 hrs in (a) November, (b) March, and (c) March for 1979 to 2010. Negative distances are MLC centers that are over snow and positive distances are MLC centers that are over ground without snow.

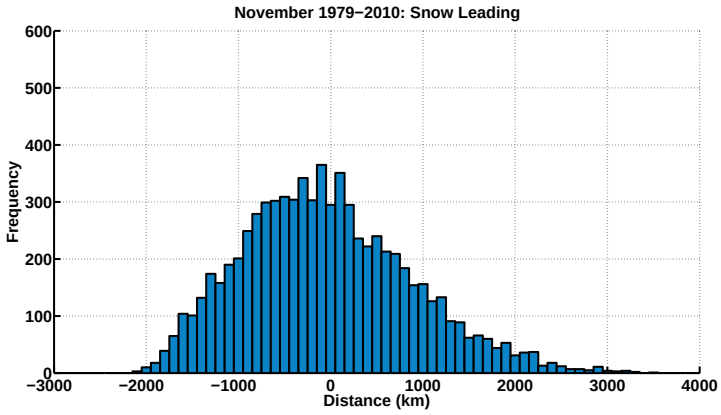

(a) Snow Leading

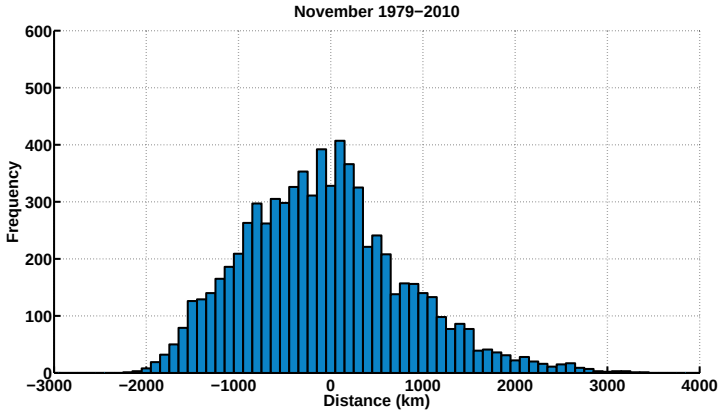

(b) No Lag

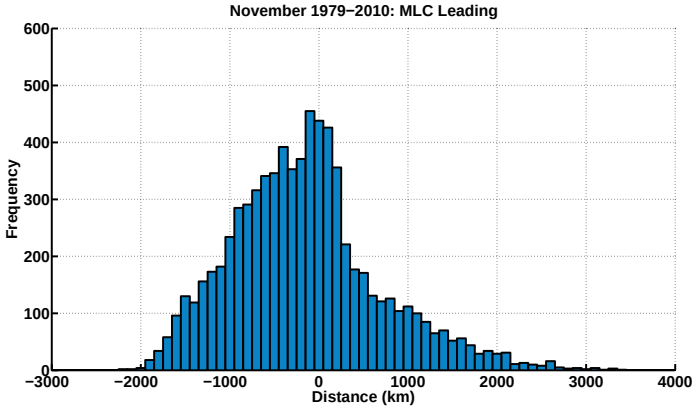

(c) MLC Leading

Figure 10: MLC center distance from snow extent for storms lasting longer than 24 hrs using various lags in November for 1979 to 2010. Negative distances are MLC centers that are over snow and positive distances are MLC centers that are over ground without snow. (a) is for snow cover leading MLC centers by two days, (b) is for snow cover and MLC centers on the same day (same as Figure 7a), and (c) is for MLC center leading snow cover by two days.

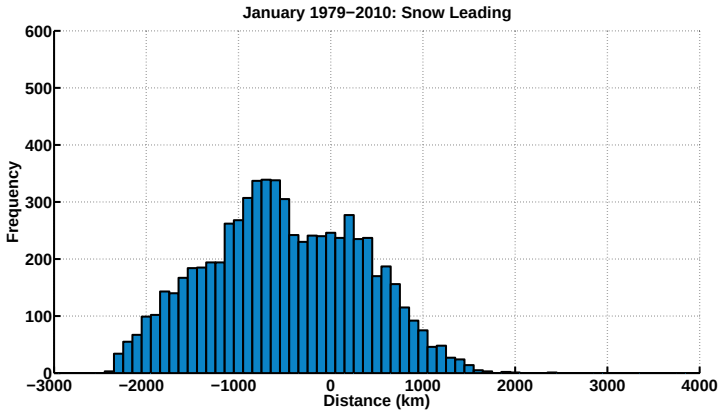

(a) Snow Leading

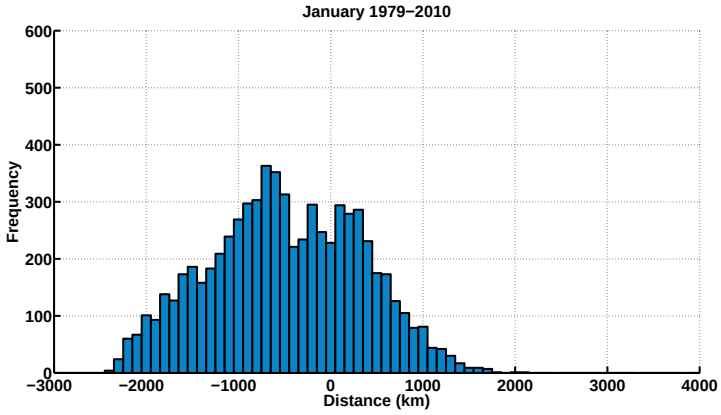

(b) No Lag

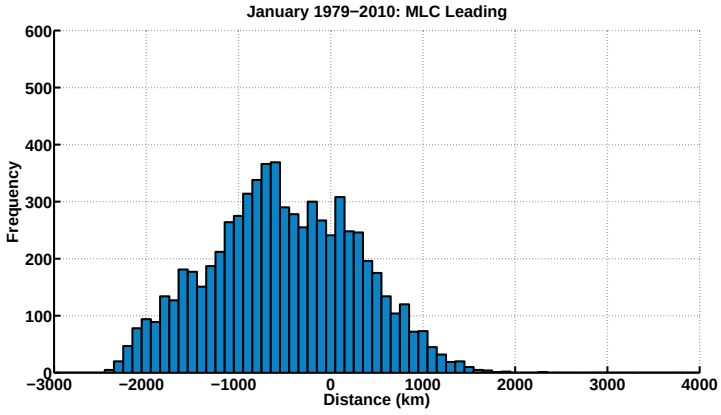

(c) MLC Leading

Figure 11: MLC center distance from snow extent for storms lasting longer than 24 hrs using various lags in January for 1979 to 2010. Negative distances are MLC centers that are over snow and positive distances are MLC centers that are over ground without snow. (a) is for snow cover leading MLC centers by two days, (b) is for snow cover and MLC centers on the same day (same as Figure 7b), and (c) is for MLC center leading snow cover by two days.

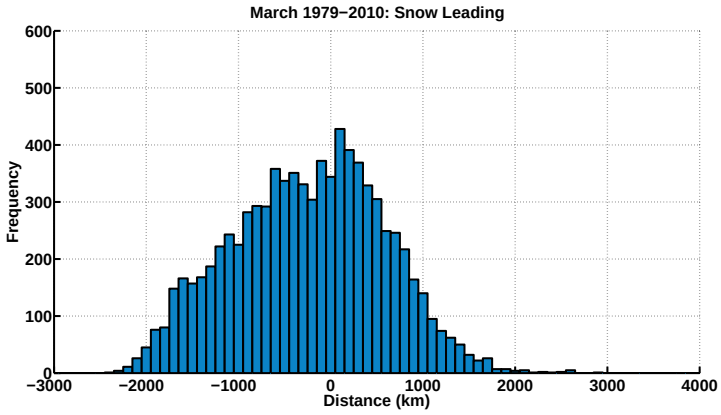

(a) Snow Leading

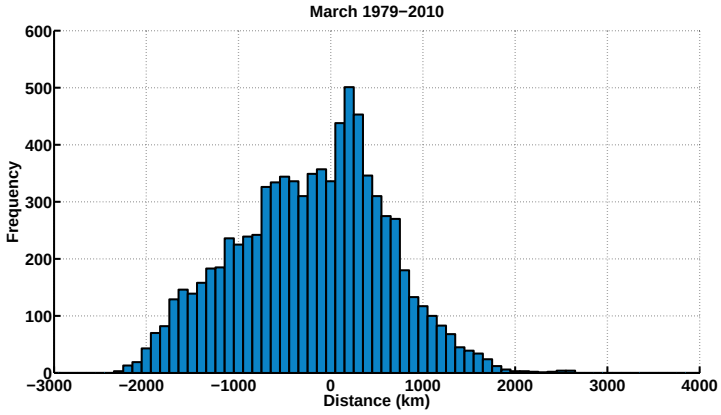

(b) No Lag

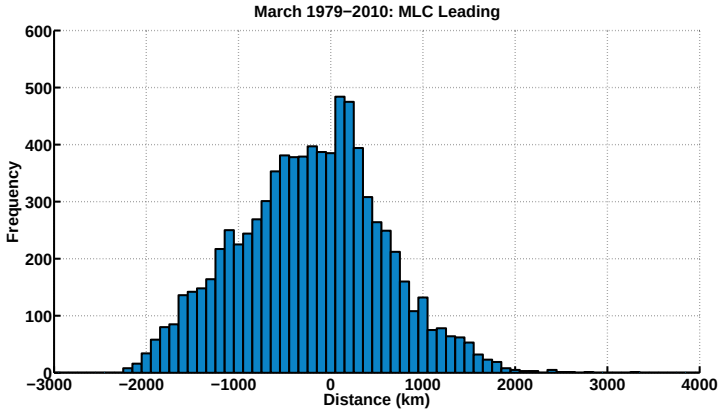

(c) MLC Leading

Figure 12: MLC center distance from snow extent for storms lasting longer than 24 hrs using various lags in March for 1979 to 2010. Negative distances are MLC centers that are over snow and positive distances are MLC centers that are over ground without snow. (a) is for snow cover leading MLC centers by two days, (b) is for snow cover and MLC centers on the same day (same as Figure 7c), and (c) is for MLC center leading snow cover by two days.

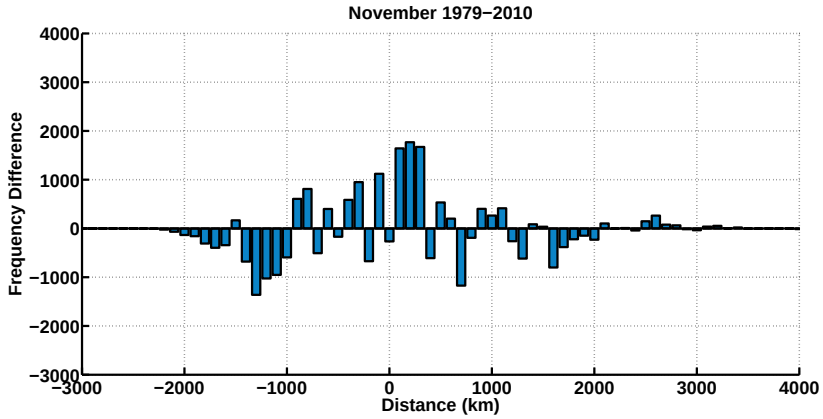

(a) November

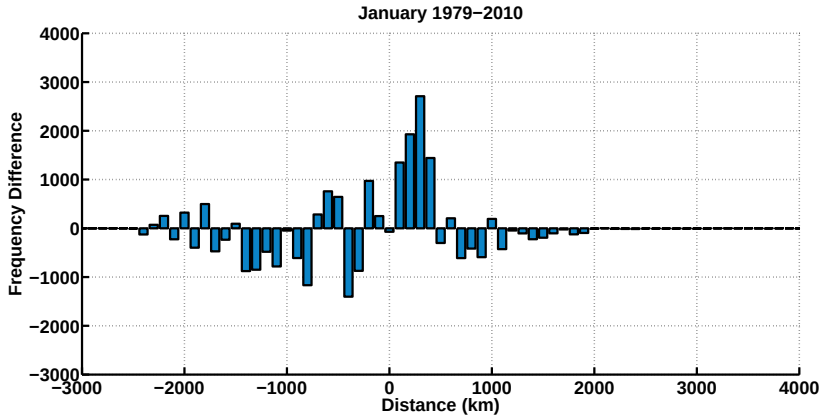

(b) January

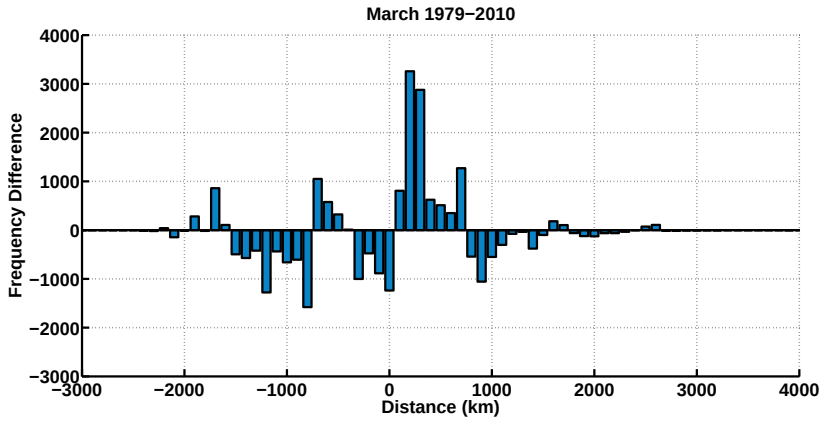

(c) March

Figure 13: The sum of the differences between the distribution for the distance between the MLC using snow for the same year and all other years. Large peaks show systematic bias caused by varying snow cover extent year.

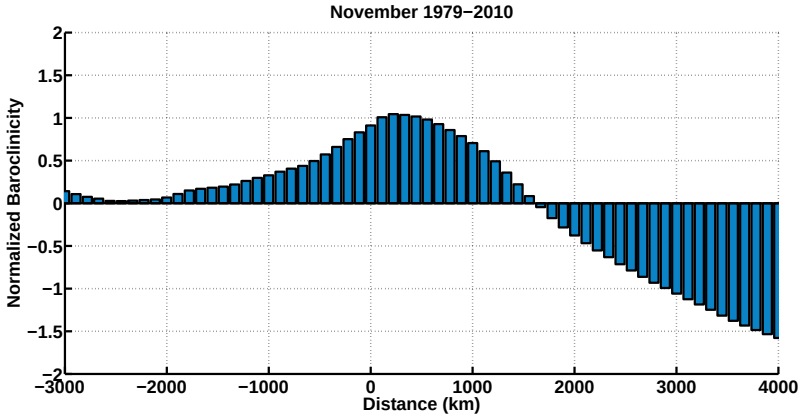

(a) November

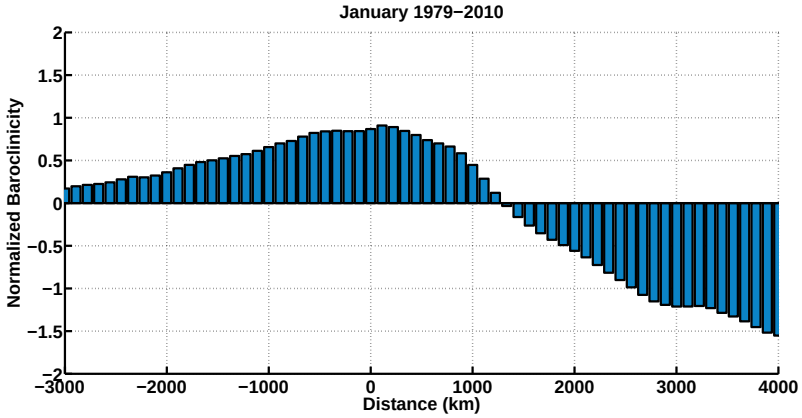

(b) January

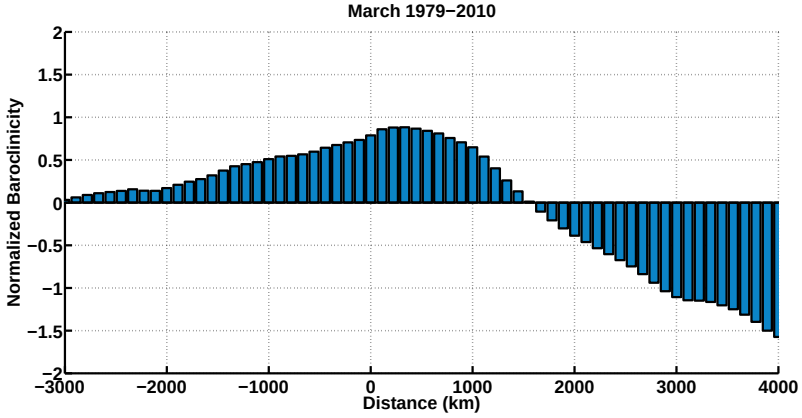

(c) March

Figure 14: Normalized low-level baroclinicity relative to the snow cover extent for (a) November, (b) January, and (c) March.

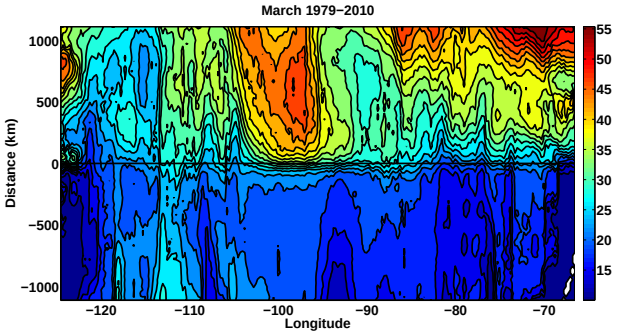

(a) Albedo

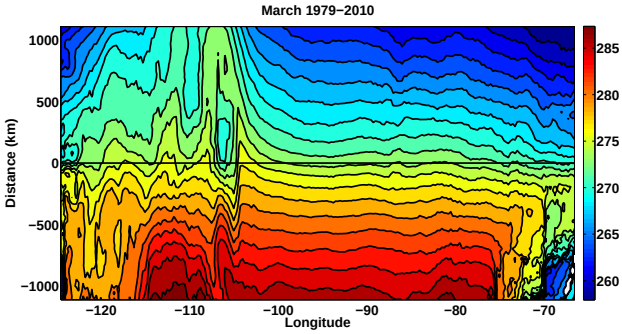

(b) 2 m Temperature

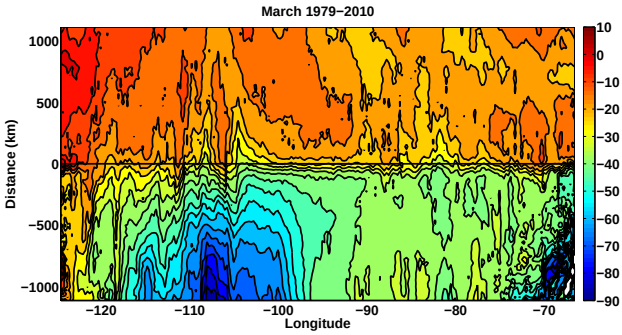

(c) Sensible Heat Flux

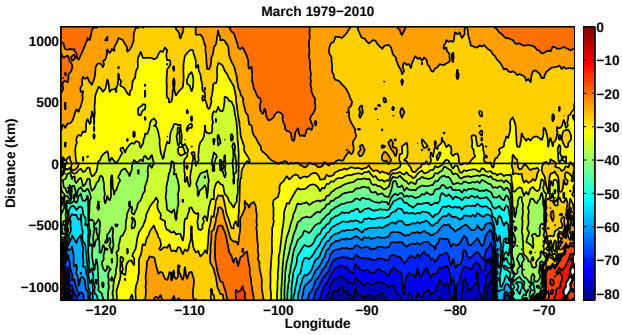

(d) Latent Heat Flux

Figure 15: Gradients of select variables relative to the cover extent (black line). (a) Surface albedo percentage, (b) 2 m air temperature (k), (c) Sensible Heat Flux (Wm^{-2}), and (d) Latent Heat Flux (Wm^{-2}). Negative fluxes are from the surface to the atmosphere.

Storms Longer than 9 hrs						
Month	Storms	Centers	Pk	BiM	M Pk (km)	ER (km)
October	4217	7489	Strong	No	100	50-250
November	3441	7417	Moderate	No	200	-150-250
December	3318	6599	Moderate	Yes	100	50-250
January	3270	6916	Weak	Yes	-600	50-350
February	3144	6602	Strong	Yes	200	50-250
March	3668	8257	Strong	No	100	50-350
April	4157	8916	Strong	No	100	50-350
May	5400	8542	Moderate	No	100	50-350
Storms Longer than 24 hrs						
Month	Storms	Centers	Pk	BiM	M Pk (km)	ER (km)
October	802	7489	Strong	No	100	50-150
November	827	7417	Moderate	No	100	-150-250
December	802	6599	Weak	No	100	none
January	798	6916	Weak	Yes	-700	50-350
February	767	6602	Moderate	No	100	50-250
March	868	8257	Strong	No	200	50-350
April	918	8916	Strong	No	100	50-350
May	920	8542	Strong	No	100	-50-250
Storms Longer than 48 hrs						
Month	Storms	Centers	Pk	BiM	M Pk (km)	ER (km)
October	199	2962	Moderate	No	100	-150-350
November	199	2813	Weak	No	-100	none
December	147	1948	Weak	No	-800	none
January	166	2335	Weak	No	-600	none
February	174	2512	Weak	No	100	none
March	218	3180	Moderate	Yes	100	50-350
April	227	3573	Moderate	No	200	50-350
May	161	2480	Moderate	No	100	50-250

Table 1: Summary statistics for MLC lasting longer than 9 hrs, 24 hrs, and 48 hrs. Peakedness (Pk) is a subjective rating of the enhancement of MLC frequency near the snow cover extent. Bimodal (BiM) distribution is a subjective determination of two distinct peaks in the distance distributions. The max peak (M Pk) is the center of the most frequent distance bin. The enhanced region (ER) is a subjective determination of where the distance distributions appear to be more pronounced as compared to a smoothly varying distribution.